

Editor-Communicated Paper

In Vitro Infection of Immortalized Primary Hepatocytes by HCV Genotype 4a and Inhibition of Virus Replication by Cyclosporin

Mohamed A. El-Farrash^{1,†}, Hussein H. Aly^{2,3,4,†}, Koichi Watashi³, Makoto Hijikata³, Hiroto Egawa², and Kunitada Shimotohno^{*,3}

¹Department of Medical Microbiology and Immunology, Faculty of Medicine, Mansoura University, Mansoura, Egypt, ²Graduate School of Medicine, Department of Transplant Surgery, Kyoto University Hospital, Kyoto, Kyoto 606–8507, Japan, ³Laboratory for Human Tumor Viruses, Institute for Virus Research, Kyoto University, Kyoto, Kyoto 606–8507, Japan, ⁴Hepatology Department, National Hepatology and Tropical Medicine Research Institute, Cairo, Egypt

Communicated by Dr. Masanobu Ohuchi: Received November 13, 2006. Accepted November 16, 2006

Abstract: Hepatitis C virus (HCV) is a major cause of liver cirrhosis and hepatocellular carcinoma worldwide. We previously reported that cyclosporin A (CsA) inhibits HCV-1b replication. However, its inhibition of JFH-1 (HCV-2a) was much less. Since HCV genotype clearly affects the *in vitro* and *in vivo* response to anti-viral therapy, we wished to examine the effect of CsA and its non-immunosuppressive derivative NIM811 on HCV genotype 4a replication. We first established an *in vitro* system supporting HCV-4a infection and replication using immortalized human hepatocytes, HuS-E7/DN24 (HuS) cells, and these cells were infected with sera obtained from Egyptian patients with chronic HCV-4a infection. HuS cells supported more robust HCV-4a replication than both HuH-7.5 and PH5CH8 cells, and HCV-4a infection and replication were completely inhibited by 3 µg/ml CsA and 0.5 µg/ml NIM811. Thus, HuS cells are a good model system supporting the infection and high-level replication of HCV-4a, and both CsA and NIM811 effectively inhibit HCV-4a replication in this system.

Key words: HCV-4a, Hepatitis, NIM811, HuS

Hepatitis C virus (HCV) is an enveloped, positive-stranded RNA virus of the genus *Hepacivirus* and family *Flaviviridae* (14). HCV is an important cause of morbidity and mortality worldwide. A high proportion of individuals infected with HCV develop chronic hepatitis, and this may progress to cirrhosis and hepatocellular carcinoma (2). The WHO estimates that there are at least 21.3 million HCV carriers in the Eastern Mediterranean countries, and this number approaches the combined estimated number of HCV carriers in the Americas (13.1 million) and Europe (8.9 million). Indeed, the prevalence of HCV infection in Egypt (15–25%) is amongst the highest in the world (18).

The genomes of a number of different HCV strains have been cloned, and the divergence of these

sequences indicates the existence of at least six HCV genotypes with a number of subtypes (12). In North America and Northern Europe, HCV subtype 1a is the most common followed by 2b and 3a. In Japan, subtype 1b is responsible for up to 73% of cases of HCV infection (13). However, genotypes other than 1, 2 or 3 represent most HCV cases in the remaining countries. HCV genotype 5 has been isolated almost exclusively from patients in South Africa, and genotype 6 is primarily found in Hong Kong, Vietnam and throughout South East Asia (13). However, it is now clear that genotype 4 is largely confined to Central Africa and the Middle East, a region containing approximately one-fifth of all HCV positive individuals worldwide (10).

Abbreviations: CsA, cyclosporin A; CyPB, cyclophilin B; HCV, hepatitis C virus; HCVpp, hepatitis C virus pseudoparticles; hTERT, human telomerase reverse transcriptase; HuS, HuS-E7/DN24; IFN- α , interferon-alpha; IRF-7, interferon regulatory factor-7; MAb, monoclonal antibody; Sv40-Lt, Simian virus 40-large T antigen.

*Address correspondence to Dr. Kunitada Shimotohno, The Institute for Virus Research, Kyoto University, 53 Kawaharacho Shogoin, Sakyo-ku, Kyoto, Kyoto 606–8507, Japan. Fax: +81-75-751-3998. E-mail: kshimoto@virus.kyoto-u.ac.jp

Our understanding of HCV was dramatically impaired by the lack of an effective virus culture system, and the establishment of self replicating full-length HCV genomic replicon systems for genotypes 1a and 1b in human hepatoma (HuH-7) cells provided valuable insight into the mechanisms of HCV replication (6). Recently, several groups reported the production of infectious virus following transfection of HCV genotype 2a genomic RNA into HuH-7 cells (1). However, immortalized, tumor derived cell lines may obscure some aspects of HCV biology, and human primary hepatocytes are the ideal cell to examine HCV replication under more physiologic conditions. Liver epithelial cells, hepatocytes and biliary cells proliferate *in vivo* in response to regenerative stimuli, but they do not proliferate under standard culture conditions *in vitro*. Recently, Aly et al. established a cell line derived from primary hepatocytes immortalized by the expression of the E6 and E7 genes of the human papillomavirus type 18 and human telomerase reverse transcriptase gene (hTERT) (1). This cell line, HuS-E7/DN24 (HuS), also lacks interferon regulatory factor-7 (IRF-7) (1), and it maintains a phenotype consistent with primary hepatocytes such as the continuous expression of albumin, apolipoprotein A, transferrin and E-cadherin without evidence of transformation even after prolonged culture (1).

At present, the only approved therapies for chronic HCV infection are interferon-alpha (IFN- α) with or without ribavirin, but these drugs fail to clear HCV from a significant number of patients (5). Recently our group discovered that cyclosporin A (CsA), and its non-immunosuppressive analogue, NIM811 could suppress HCV genome replication in a cell culture system (4, 16). The anti-HCV effects of CsA correlated with cyclophilin B inhibition (CyPB). CyPB, a cellular target of CsA, regulates HCV replication through its interaction with the viral RNA-dependent RNA polymerase NS5B, and CsA suppresses HCV replication by disrupting the association of CyPB with NS5B (17). CsA strongly suppressed HCV-1b replication, but its effects on HCV-2a (JFH-1) replication were less profound, indicating that different HCV genotypes may be differentially susceptible to CsA (17). However, the ability of CsA to inhibit the replication of HCV-4a, one of the most common genotypes worldwide, has not been reported.

We infected HuS immortalized primary hepatocytes with serum samples obtained from Egyptian patients with chronic HCV-4a infection and examined the ability of CsA and NIM811 to suppress viral replication. Our data indicate that HCV-4a is highly susceptible to CsA and NIM811 treatment, suggesting that these may rep-

resent new treatment options to explore in HCV-4a infected individuals.

Materials and Methods

Cells. The immortalized primary hepatocyte cell line HuS-E7/DN24 (HuS) was cultured as reported (1). The hepatoma cell line HuH-7.5 that supports infection and replication of the recombinant HCV strain JFH-1 (HCV-2a) (15) was cultured as previously described. Simian virus 40-large T antigen (Sv40-Lt) immortalized primary hepatocytes (PH5CH8) supporting infection and replication of HCV-1b genotype samples were cultured as reported (16).

Serum samples. Serum samples from Egyptian patients with chronic HCV hepatitis genotype 4a were collected in Egypt (after approval of the Medical Research Ethics Committee in Mansoura University). The virus titer in sera was determined using real-time PCR for the detection of HCV as described (8).

Real-time reverse transcriptase polymerase chain reaction (real-time RT-PCR) analysis. Five-hundred nanograms of total RNA isolated from cells was reverse transcribed as previously described (1), and the 5'-untranslated region of HCV genomic RNA was quantitated using the ABI PRISM 7700 sequence detector (Applied Biosystems, Foster City, Calif., U.S.A.) as described previously (8). The forward and reverse primers used in this experiment were 5'-CGGGA-GAGCCATAGTGG-3' and 5'-AGTACCACAAGGC-CITTCG-3', respectively. The fluorogenic probe was 5'-CTGCGGAACCGGTGAGTACAC-3'. As an internal control, ribosomal RNA was also quantified using *TaqMan* ribosomal RNA control reagents (Applied Biosystems).

Chemicals. CsA and IFN- α were purchased from Sigma and Otsuka Pharmaceutical Co., respectively. NIM811 was generously provided by Novartis (Basel, Switzerland).

In vitro infection experiments. HuS, PH5CH8 and HuH-7.5 cells were harvested, washed, adjusted to 5×10^4 cells/ml in growth medium and cultured in 12-well plates with 1 ml media per well. After 24 hr, the culture medium was replaced with 1 ml of complete medium containing HCV. Plates were incubated at 37 C for 24 hr, and the virus-containing media was removed. The cells were then washed twice with PBS, and 1 ml of complete culture medium was added to each well. Plates were re-incubated and the cells were harvested at the indicated times for evaluation. Total RNA was extracted from infected or non-infected cells, and HCV-RNA was measured by real time RT-PCR as described (8).

HCV infection neutralization experiment. HCV infection of HuS cells was inhibited using anti-CD81 (BD-Bioscience) or anti-HCV-E2 (AP33) as previously reported (7). The mouse monoclonal antibody (MAb) AP33 recognizes the E2 glycoprotein of HCV-1A, and it neutralizes retroviral pseudoparticles (HCVpp) carrying genetically diverse HCV envelope glycoproteins, including HCV-4a-glycoproteins (9). Anti-tubulin (Sigma, St. Louis, Mo., U.S.A.) was used as a control.

Inhibition of HCV replication. HuS cells were cultured at a concentration of 5×10^4 cells/well in 12-well plates. After 24 hr, cells were infected by adding growth medium containing HCV-4a serum (adjusted to a final virus titer of 5×10^4 copies of RNA/ml) and the

indicated concentrations of CsA, NIM811, or IFN- α . Plates were incubated at 37 C for 24 hr, and the medium was then removed, the cells were washed twice with PBS, and 1 ml of fresh medium containing CsA, NIM811, or IFN- α was added to the cells. On day 5 post-infection, the medium was removed, and the cells were washed, trypsinized and collected. Total RNA was extracted from infected or non-infected cells, and HCV-RNA was measured by real-time RT-PCR.

CsA and NIM811 toxicity test. HuS cells were cultured at a concentration of 5×10^4 cells/well in 12-well plates. Cells were untreated, or treated with 3 μ g/ml CsA or 1 μ g/ml NIM811. Every 2 days, the medium was replaced with fresh, drug-containing medium.

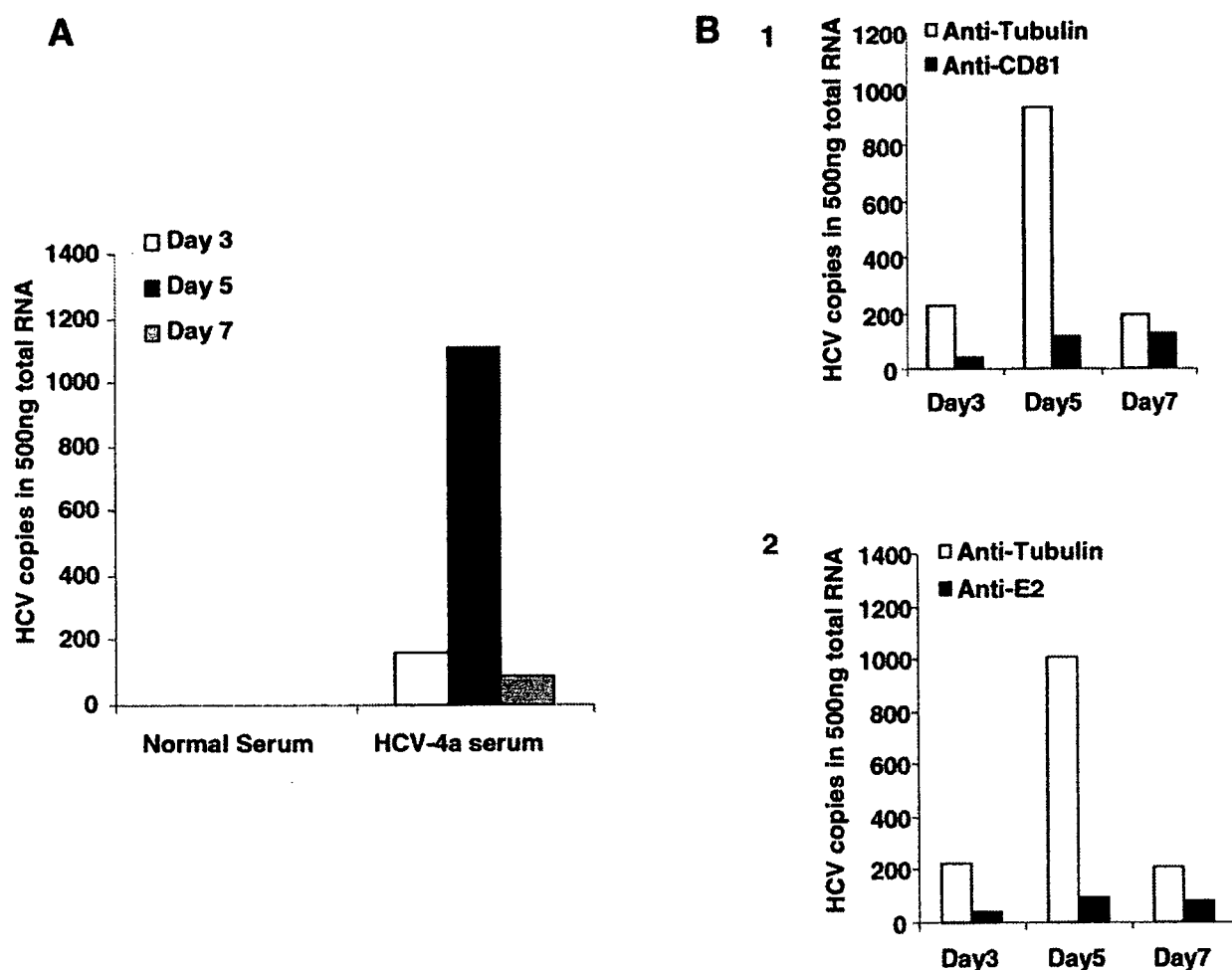


Fig. 1. Kinetics of HCV-4a replication in HuS-E7/DN24 (HuS) cells. (A) Cells were incubated with a serum sample containing HCV-4a virus for 24 hr, and the virus-containing medium was then removed, the cells were washed twice and incubated for the indicated periods of time. At 3, 5 and 7 days after infection, cells were washed again, and total RNA was extracted and used to determine the number of HCV-RNA copies after reverse transcription and real-time PCR. The results shown are the average of two independent experiments. (B) Cells were treated with anti-CD81 or anti-tubulin antibody (1), or HCV containing serum was pre-incubated with anti-E2 or anti-tubulin antibody (2). HCV-4a infection was performed and analyzed as above. The results shown are the average of two independent experiments.

Wells from each group were collected on days 1, 2, 3, 4, and 5 to examine the number of viable cells in each well after staining of the cells with trypan blue.

Results

HCV-4a Infection and Kinetics in HuS Cells in Vitro

We previously established the HuS cell line and showed that these cells were efficiently infected with HCV-1b and HCV-2b containing serum and JFH-1 (HCV-2a) concentrated medium (1). To determine whether HuS cells could support HCV-4a infection, HCV-4a containing serum was incubated with HuS cells for 24 hr, and, following washing and a change of media, the cells were harvested 3, 5, and 7 days after infection. Total RNA was extracted from the infected cells, and the amount of HCV-RNA in 500 ng total RNA was measured (Fig. 1A). As expected, after 3 days in culture the RNA extracted from non-infected HuS cells did not contain any HCV copies. However, viral RNA was detected in cells incubated with HCV-4a containing serum. The number of viral genomes detected was 164.5 ± 52 copies/500 ng of total RNA at day 3, and this peaked at $1,111 \pm 176$ copies/500 ng of total RNA at day 5. The increase from day 3 to day 5 after infection clearly indicates viral replication occurring in these cells rather than increased viral entry without replication. The number of viral genomes decreased dramatically on day 7 to 80 ± 18 copies/500

ng of total RNA. Identical results were obtained using HCV-4a genotype samples isolated from two other individuals (data not shown).

HCV-4a Infection Is Neutralized by Anti-CD81 and Anti-E2

CD81 is involved in the entry of HCV pseudoparticles and *in vitro*-synthesized JFH-1 (15). Similarly, HCV envelope protein E2 is essential for HCV cell entry and infection (7). Blocking antibodies against both CD81 and E2 inhibit viral infection in *in vitro* models. To determine if HCV-4a infection of HuS cells is analogous to previously described systems, we treated cells with either anti-CD81 (Fig. 1B-1) or anti-HCV-E2 (Fig. 1B-2) blocking antibodies. Consistent with results obtained using other HCV genotypes, antibodies against CD81 and HCV-E2 effectively reduced HCV-4a infectivity of HuS cells compared with a non-blocking anti-tubulin antibody.

HuS Cells Are More Permissive to Infection by HCV-4a than PH5CH8 and HuH-7.5 Cells

HuS cells clearly support HCV-4a infection and replication. We wished to compare the ability of different cell lines to support infection and replication of HCV-4a. HuS, PH5CH8 and HuH-7.5 cells were infected with HCV-4a serum containing 5.0×10^4 copies/ml, and the number of viral copies at 3, 5, and 7 days after infection was examined. PH5CH8 and HuH-

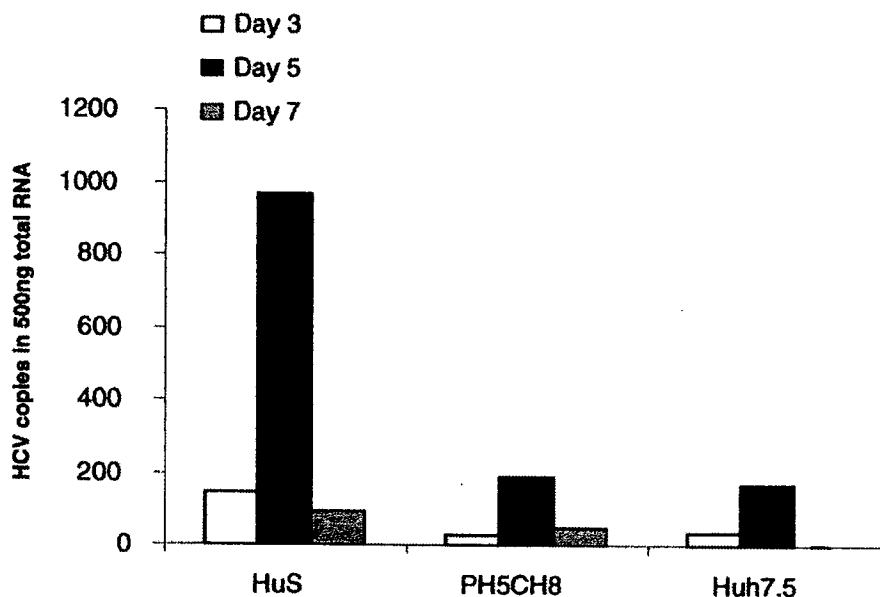


Fig. 2. HuS cells are more permissive to infection by HCV-4a than PH5CH8 and HuH-7.5 cells. HCV-4a replication was examined in HuS cells, PH5CH8 and HuH-7.5 cells. HuS, PH5CH8, and HuH-7.5 cells were infected with the same serum sample under the same conditions, and the extent of HCV genome replication was measured by real-time RT-PCR on days 3, 5, and 7 after infection. The results shown are the average of two independent experiments.

HuH-7.5 cells supported HCV-4a infection to some extent, but much less viral replication occurred in these cells (Fig. 2). Indeed, we would not detect any HCV RNA in HuH-7.5 cells 7 days after infection. Identical results were obtained using HCV-4a genotype virus isolated from two other individuals (data not shown). These data are consistent with a previous report showing increased viral infection and/or replication in HuS cells incubated with HCV genotypes 1b and 2b derived from patients' sera (1).

Inhibition of HCV-4a Replication in HuS Cells by CsA and NIM811

Having established that HuS cells support HCV-4a infection and replication similar to other HCV genotypes examined, we wished to determine if HCV-4a

was sensitive to treatment with CsA or its non-immunosuppressive derivative NIM811. Serum isolated from two different individuals was used as a source of HCV-4a for all experiments. For both samples, treatment of infected HuS cells with 1 $\mu\text{g/ml}$ of CsA reduced the number of recovered viral copies by 75% at 5 days compared with untreated cells, and increasing the concentration of CsA to 3 $\mu\text{g/ml}$ almost completely inhibited HCV-4a replication in HuS cells (Fig. 3A). Furthermore, we were unable to detect any viral RNA in HCV-4a infected HuS cells treated with either 0.5 or 1 $\mu\text{g/ml}$ NIM811 (Fig. 3B). For comparison, we also treated infected cells with 50 IU/ml IFN- α , and this reduced viral replication by 80–90% in HuS cells (Fig. 3C). The inhibition of HCV-4a replication by CsA or NIM811 could be due to a general cytotoxic effect, and,

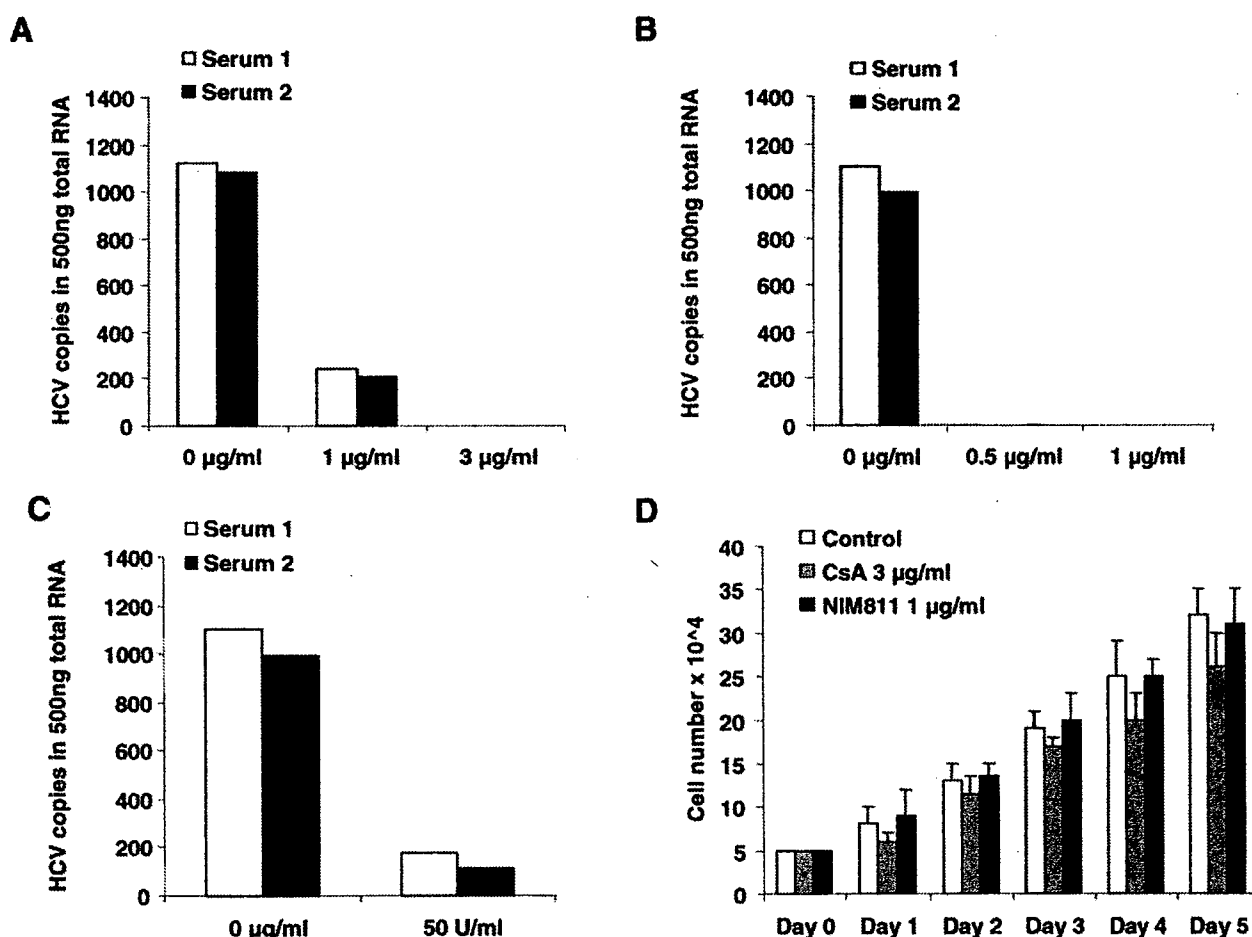


Fig. 3. Inhibition of HCV-4a replication in HuS cells by cyclosporin and NIM811. Two different serum samples containing HCV-4a were used to infect HuS cells in presence of CsA 0, 1 or 3 $\mu\text{g/ml}$ (A), NIM811 0, 0.5 or 1 $\mu\text{g/ml}$ (B) and IFN- α 0 or 50 IU/ml (C). Cells were incubated for 5 days and the level of HCV replication was measured by real-time RT-PCR as described in Fig. 1. The results represent the average of two independent experiments. (D) HuS cells were left untreated or treated with either 3 $\mu\text{g/ml}$ CsA or 1 $\mu\text{g/ml}$ NIM811 for 5 days. Cells were harvested at the indicated times, and the number of viable cells in each well was determined. The results shown are the average of 3 independent experiments.

to exclude this possibility, we cultured HuS cells with or without CsA or NIM811 for 5 days. Although HuS cell proliferation was slightly reduced by the inclusion 3 $\mu\text{g/ml}$ of CsA in the culture media, it was not affected by the addition of 1 $\mu\text{g/ml}$ of NIM811 compared to control untreated cells (Fig. 3D). Thus, the inhibition of HCV-4a replication by NIM811 and CsA in HuS cells appear to be due to direct anti-viral effects.

Discussion

There are six major HCV genotypes with a number of different subtypes that vary by geographic distribution and mode of transmission (12). Subtypes 1a, 1b, 2a, 2b, and 3a are distributed globally and account for the majority of HCV infections worldwide (13). HCV-4a is the predominant genotype seen in the Middle East, a region encompassing approximately 20% of the estimated 170 million HCV carriers in the world (11). HCV-4a responds poorly to interferon treatment, and individuals infected with HCV-4a are at higher risk of liver related death and the need for transplantation (19). Thus, the development of new treatments that are effective across a broader range of HCV genotypes is urgently needed.

The development of more effective antiviral therapies and an effective HCV vaccine remain the largest challenges for HCV research in the near future. However, because HCV genotype affects the outcome of antiviral therapy, it has become increasingly clear that an *in vitro* system supporting HCV-4a infection and replication is needed to develop anti-viral therapies effective against this important viral subtype. Recent studies have examined several different viral genotypes using the replicon system in HuH-7 cells, but this is the first report specifically designed to determine *in vitro* conditions compatible with HCV-4a infection and replication.

We recently established the HuS cell line, and this cell line is able to be infected *in vitro* by sera containing HCV-1b and -2b (1). In this study, we showed that HuS cells also clearly support the infection and replication of HCV-4a derived from patient serum samples. A high level of HCV-RNA was seen in these cells 5 days after infection, but this rapidly declined by day 7. The kinetics of infection observed for HCV-4a in HuS cells was similar to that observed when PH5CH8 cells were infected with HCV-1b containing plasma (16). Since the aim of this paper was to study the suppressive effect of CsA and NIM811 on HCV infection and replication, which was monitored clearly on days 3 and 5, we didn't culture the infected cells for more than 7 days. The extent of HCV-4a infection of HuS was much greater

than that for the PH5CH8 and HuH-7.5 cell lines, and these differences in permissiveness may arise from the relative amounts or activities of host cell factors required for RNA replication. Alternatively, HuS cells lack functioning IRF-7, and this likely impairs their ability to produce IFN- α . The absence IFN- α from the culture media following infection could clearly contribute to the increased replication seen in HuS cells.

There is an urgent need for improved HCV drug therapies. We previously reported that CsA suppresses HCV replication *in vitro* (16), and these effects are also seen using its non-immunosuppressive derivative NIM811. These compounds can induce multiple-log reductions in HCV-RNA levels in a replicon cell culture system using HCV-1b genotype virus (4). However, the ability of CsA to inhibit a HCV-2a genotype virus, JFH-1, was greatly reduced. In this study we examined the effects of CsA and NIM811 on HCV-4a infection and replication in HuS cells. As was seen with HCV-1b, both CsA and NIM811 strongly inhibited HCV-4a infection and replication in HuS cells. Furthermore, the inhibition by NIM811 was much greater at lower doses than that seen for CsA. These findings were similar to those previously reported for HuH-7 cells harboring a HCV-1b replicon (4).

The HuS cell line is the only system described available for the study of HCV-4a infection and replication. Using this cell line, we showed that HCV-4a replication is impaired by CsA and to a greater extent by its non-immunosuppressive derivative NIM811. Despite these findings, more studies are clearly needed to determine the activity of these drugs *in vivo* as well as characterize the possible differences in the HCV-4a life-cycle.

The CsA derivative, NIM811 was kindly provided by Novartis (Basel, Switzerland). This work was supported by Grants-in-Aid for cancer research and for the second-term comprehensive 10-year strategies for cancer control from the Ministry of Health, Labour and Welfare, Japan, by Grants-in-Aid for scientific research from the Ministry of Education, Culture, Sports, Science and Technology, Japan, by Grants-in-Aid for the research for the future program from the Japan Society for the Promotion of Science. Dr. M.A. El-Farrash (Ph.D.) was a recipient of the JSPS Invitation Fellowship Programs for Research in Japan. Dr. Hussein H. Aly is a recipient of the Japanese Gakushu Shoreihi scholarship and was partly supported by the Prof. Yassin A. El Ghaffar memorial scholarship for the improvement of liver research in Egypt.

References

- 1) Aly, H.H., Watashi, K., Hijikata, M., Kaneko, H., Takada, Y., Egawa, H., Uemoto, S., and Shimotohno, K. 2007. Serum-derived hepatitis C virus infectivity in interferon regulatory factor-7-suppressed human primary hepatocytes.

- J. Hepatol.* **46**: 26–36
- 2) Chen, S.L., and Morgan, T.R. 2006. The natural history of hepatitis C virus (HCV) infection. *Int. J. Med. Sci.* **3**(2): 47–52.
 - 3) Choo, Q.L., Kuo, G., Weiner, A.J., Overby, L.R., Bradley, D.W., and Houghton, M. 1989. Isolation of a cDNA clone derived from a blood-borne non-A, non-B viral hepatitis genome. *Science* **244**: 359–362.
 - 4) Goto, K., Watashi, K., Murata, T., Hishiki, T., Hijikata, M., and Shimotohno, K. 2006. Evaluation of the anti-hepatitis C virus effects of cyclophilin inhibitors, cyclosporin A, and NIM811. *Biochem. Biophys. Res. Commun.* **343**: 879–884.
 - 5) Huang, R.H., and Hu, K.Q. 2006. A practical approach to managing patients with HCV infection. *Int. J. Med. Sci.* **3**(2): 63–68.
 - 6) Lohmann, V., Körner, F., Koch, J.O., Herian, U., Theilmann, L., and Bartenschlager, R. 1999. Replication of subgenomic hepatitis C virus RNAs in a hepatoma cell line. *Science* **285**: 110–113.
 - 7) McKeating, J.A., Zhang, L.Q., Logvinoff, C., Flint, M., Zhang, J., Yu, J., Butera, D., Ho, D.D., Dustin, L.B., Rice, C.M., and Balfe, P. 2004. Diverse hepatitis C virus glycoproteins mediate viral infection in a CD81-dependent manner. *J. Virol.* **78**: 8496–8505.
 - 8) Murata, T., Ohshima, T., Yamaji, M., Hosaka, M., Miyanari, W., Hijikata, M., and Shimotohno, K. 2005. Suppression of HCV virus replication by TGF-beta. *Virology* **331**: 407–417.
 - 9) Owsianka, A., Tarr, A.W., Juttla, V.S., Lavillette, D., Bartosch, B., Cosset, F.L., Ball, J.K., and Patel, A.H. 2005. Monoclonal antibody AP33 defines a broadly neutralizing epitope on the hepatitis C virus E2 envelope glycoprotein. *J. Virol.* **79**: 11095–11104.
 - 10) Ray, S.C., Arthur, R.R., Carella, A., Bukh, J., and Thomas, D.L. 2000. Genetic epidemiology of hepatitis C virus throughout Egypt. *J. Infect. Dis.* **182**: 698–707.
 - 11) Ramia, S., and Eid-Fares, J. 2006. Distribution of hepatitis C virus genotypes in the Middle East. *Int. J. Infect. Dis.* **10**: 272–277.
 - 12) Simmonds, P., Holmes, E.C., Cha, T.A., Chan, S.W., McOmish, F., Irvine, B., Beall, E., Yap, P.L., Kolberg, J., and Urdea, M.S. 1993. Classification of hepatitis C virus into six major genotypes and a series of subtypes by phylogenetic analysis of the NS-5 region. *J. Gen. Virol.* **74**: 2391–2399.
 - 13) Theodore, S.Y., and Jamal, M.M. 2006. Epidemiology of hepatitis C virus (HCV) infection. *Int. J. Med. Sci.* **3**(2): 41–46.
 - 14) Van Regenmortel, M.H.V., Fauquet, C.M., Bishop, D.H.L., Carstens, E.B., Estes, M.K., Lemon, S.M., Maniloff, J., Mayo, M.A., McGeoch, D.J., Pringle, C.R., and Wickner, R.B. 2000. Virus taxonomy: the seventh report of the International Committee on Taxonomy of Viruses, Academic Press, San Diego.
 - 15) Wakita, T., Pietschmann, T., Kato, T., Date, T., Miyamoto, M., Zhao, Z., Murthy, K., Habermann, A., Krausslich, H.G., Mizokami, M., Bartenschlager, R., and Liang, T.J. 2005. Production of infectious hepatitis C virus in tissue culture from a cloned viral genome. *Nat. Med.* **11**: 791–796.
 - 16) Watashi, K., Hijikata, M., Hosaka, M., Yamaji, M., and Shimotohno, K. 2003. Cyclosporin A suppresses replication of hepatitis C virus genome in cultured hepatocytes. *Hepatology* **38**: 1282–1288.
 - 17) Watashi, K., Ishii, N., Hijikata, M., Inoue, D., Murata, T., Miyanari, Y., and Shimotohno, K. 2005. Cyclophilin B is a functional regulator of hepatitis C virus RNA polymerase. *Mol. Cell* **19**: 111–122.
 - 18) WHO. 1999. Global surveillance and control of hepatitis C. Report of a WHO Consultation organized in collaboration with the Viral Hepatitis Prevention Board, Antwerp, Belgium. *J. Viral Hepat.* **6**: 35–47.
 - 19) Zylberberg, H., Chaix, M.L., and Brechot, C. 2000. Infection with hepatitis C virus genotype 4 is associated with a poor response to interferon-alpha [Letter]. *Ann. Intern. Med.* **132**: 845–846.

The lipid droplet is an important organelle for hepatitis C virus production

Yusuke Miyanari^{1,2}, Kimie Atsuzawa³, Nobuteru Usuda³, Koichi Watashi^{1,2}, Takayuki Hishiki^{1,2}, Margarita Zayas⁴, Ralf Bartenschlager⁴, Takaji Wakita⁵, Makoto Hijikata^{1,2} and Kunitada Shimotohno^{1,2,6}

The lipid droplet (LD) is an organelle that is used for the storage of neutral lipids. It dynamically moves through the cytoplasm, interacting with other organelles, including the endoplasmic reticulum (ER)^{1–3}. These interactions are thought to facilitate the transport of lipids and proteins to other organelles. The hepatitis C virus (HCV) is a causative agent of chronic liver diseases⁴. HCV capsid protein (Core) associates with the LD⁵, envelope proteins E1 and E2 reside in the ER lumen⁶, and the viral replicase is assumed to localize on ER-derived membranes. How and where HCV particles are assembled, however, is poorly understood. Here, we show that the LD is involved in the production of infectious virus particles. We demonstrate that Core recruits nonstructural (NS) proteins and replication complexes to LD-associated membranes, and that this recruitment is critical for producing infectious viruses. Furthermore, virus particles were observed in close proximity to LDs, indicating that some steps of virus assembly take place around LDs. This study reveals a novel function of LDs in the assembly of infectious HCV and provides a new perspective on how viruses usurp cellular functions.

Hepatitis C virus (HCV) has a plus-strand RNA genome that encodes the viral structural proteins Core, E1 and E2, the p7, and the nonstructural (NS) proteins 2, 3, 4A, 4B, 5A and 5B (refs 7, 8). NS proteins are reported to localize on the cytoplasmic side of endoplasmic reticulum (ER) membranes⁹. To elucidate the mechanisms of virus production, we used a HCV strain, JFH1, which can produce infectious viruses^{10–12}. We first investigated the subcellular localization of the HCV proteins in cells that had been transfected with JFH1^{E2FL} RNA, in which a part of the hypervariable region 1 of E2 was replaced by the FLAG epitope tag (see Supplementary Information, Fig. S1, S2a–d). Core localized to the lipid droplets (LDs; Fig. 1a), as previously reported⁵. Interestingly, NS proteins were also detected around LDs in 60–90% of JFH1^{E2FL}-replicating cells (Fig. 1a, c). Similar levels of colocalization of LDs with viral proteins were observed in cells that had been transfected with chimeric HCV genomes

expressing structural proteins, p7 and part of NS2 of the genotype 1b (Con1) or the genotype 1a (H77) isolate (see Supplementary Information, Fig. S1, S2e)¹³. In contrast, there was no close association between the LDs and NS proteins in cells that had been transfected with JFH1^{dC3} RNA (Fig. 1b, c), which lacked the coding region of Core (Supplementary Information, Fig. S1). NS proteins were diffusely present on the ER, suggesting that NS proteins are translocated from the ER to LDs in JFH1^{E2FL}-replicating cells in a Core-dependent manner. Importantly, there was no association between LDs and PDI, an ER marker protein, indicating that either ER membranes were absent in close proximity to LDs or that PDI was excluded from such membranes (Fig. 1c). These results were supported by western blot analysis of the LD fraction (Fig. 1d). The LD fraction contained ADRP, an LD marker, but not the ER markers Calnexin and Grp78 (data not shown), indicating that there was no ER contamination in the LD fraction. However, the LD fraction from JFH1^{E2FL}-replicating cells contained high levels of viral proteins in contrast to the LD fraction from JFH1^{dC3}-replicating cells (in which HCV proteins were virtually absent (Fig. 1d, LD fraction)), even though the expression levels of the NS proteins in whole-cell extracts were similar (Fig. 1d, whole-cell extract). About 20–45% of the total HCV proteins associated with the LDs in JFH1^{E2FL}-replicating cells (Fig. 1e). Consistent with previous reports that Core enhances the formation of LDs¹⁴, overproduction of LDs was observed in JFH1^{E2FL}-, but not JFH1^{dC3}-replicating cells (Supplementary Information, Fig. S3a–l). Treatment of the cells with oleic acid, which enhanced the formation of LDs, did not affect either HCV protein levels or the recruitment of viral proteins to LDs in JFH1^{dC3}-replicating cells (Supplementary Information, Fig. S3m–p). Thus, the overproduction of LDs is insufficient for the recruitment of HCV proteins to LDs. To examine the ability of Core to recruit NS proteins to LDs, JFH1^{dC3}-replicating cells were transfected with a plasmid-expressing Core (Core^{Wt}) (Fig. 1f, g). NS5A accumulated around LDs (Fig. 1f, arrowheads and panel 2), as did NS3 and NS4AB (Fig. 1g), in cells expressing Core^{Wt}. The translocation of NS proteins to LDs was, however, not observed in JFH1^{dC3}-replicating cells expressing Core^{pp1AA} (Fig. 1g and Supplementary Information, Fig. S2f–h),

¹Department of Viral Oncology, Institute for Virus Research, Kyoto University, Kyoto 606-8507, Japan; ²Graduate School of Biostudies, Kyoto University, Kyoto 606-8507, Japan; ³Department of Anatomy, Fujita Health University School of Medicine, Toyoake 470-1192, Japan; ⁴Department of Molecular Virology, University of Heidelberg, 69120 Heidelberg, Germany; ⁵Department of Virology II, National Institute of Infectious Diseases, Tokyo 162-8640, Japan
⁶Correspondence should be addressed to K.S. (e-mail: shimkuni@z8.keio.jp)

Received 16 March 2007; accepted 31 July 2007; published online 26 August 2007; DOI: 10.1038/ncb1631

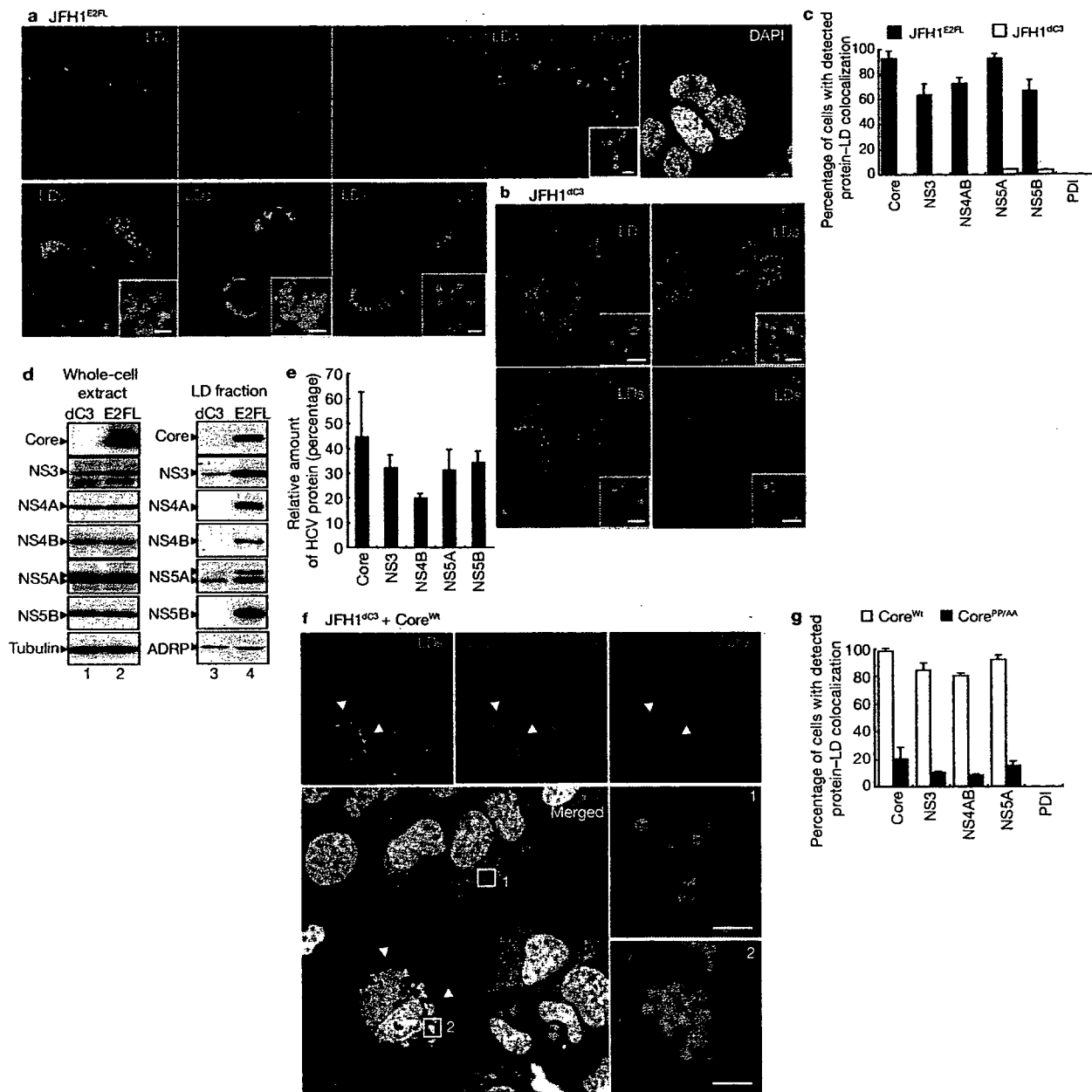


Figure 1 Core recruits NS proteins to LDs. (a) Huh-7 cells transfected with JFH1^{E2FL} RNA were labelled with antibodies against Core (red), NS5A (blue), NS3 (red), NS4AB (red) or NS5B (red). Lipid droplets (LDs) and nuclei were stained with BODIPY 493/503 (green) and DAPI (white in upper panel, blue in lower panels), respectively. Insets are high magnification images of areas in the respective panel. (b) JFH1^{dC3} replicon-bearing cells were labelled with DAPI (blue), BODIPY 493/503 (green) and indicated antibodies (red). The insets are high magnifications of the corresponding panel. (c) Percentages of JFH1^{E2FL}- or JFH1^{dC3}-bearing cells in which hepatitis C virus (HCV) proteins or PDI colocalize with LDs ($n > 200$). (d) Western blot analysis of HCV proteins and marker proteins in whole-cell extracts and the LD fractions from cells transfected with JFH1^{E2FL} (E2FL) or JFH1^{dC3} (dC3) RNA. (e) HCV proteins were quantified by using

western blotting data of the purified LD fraction and whole-cell extracts of JFH1^{E2FL}-replicating cells. Results are shown as relative amounts of HCV proteins co-fractionated with LDs. This results correspond well with results obtained by quantitative immunofluorescence staining (data not shown). (f) Trans-complementation with Core^{WT} relocates NS proteins to LDs. JFH1^{dC3} replicon-bearing cells were transfected with pcDNA3-Core^{WT} and labelled with BODIPY 493/503 (green), DAPI (white) and antibodies against NS5A (red) and Core (blue). Arrowheads indicate Core^{WT}-expressing cells. Higher-magnification images of area 1 and area 2 are shown in panels 1 and 2, respectively. Scale bars, 2 μ m. (g) The percentages of cells in which HCV proteins colocalize with LDs in the presence of Core^{WT} or Core^{PP3AA} ($n > 200$). Uncropped images of gels are shown in Supplementary Information Fig. S6. All error bars are derived from s.d.

a variant of Core containing two alanine substitutions at amino-acid positions 138 and 143 that fails to associate with LDs¹⁵. These results show that LD-associated Core recruits NS proteins from the ER to LDs.

Next, we investigated whether Core also recruited HCV RNA to LDs. *In situ* hybridization analysis showed that in more than 80% of JFH1^{E2FL}-replicating cells, both plus- and minus-strand RNAs were diffusely

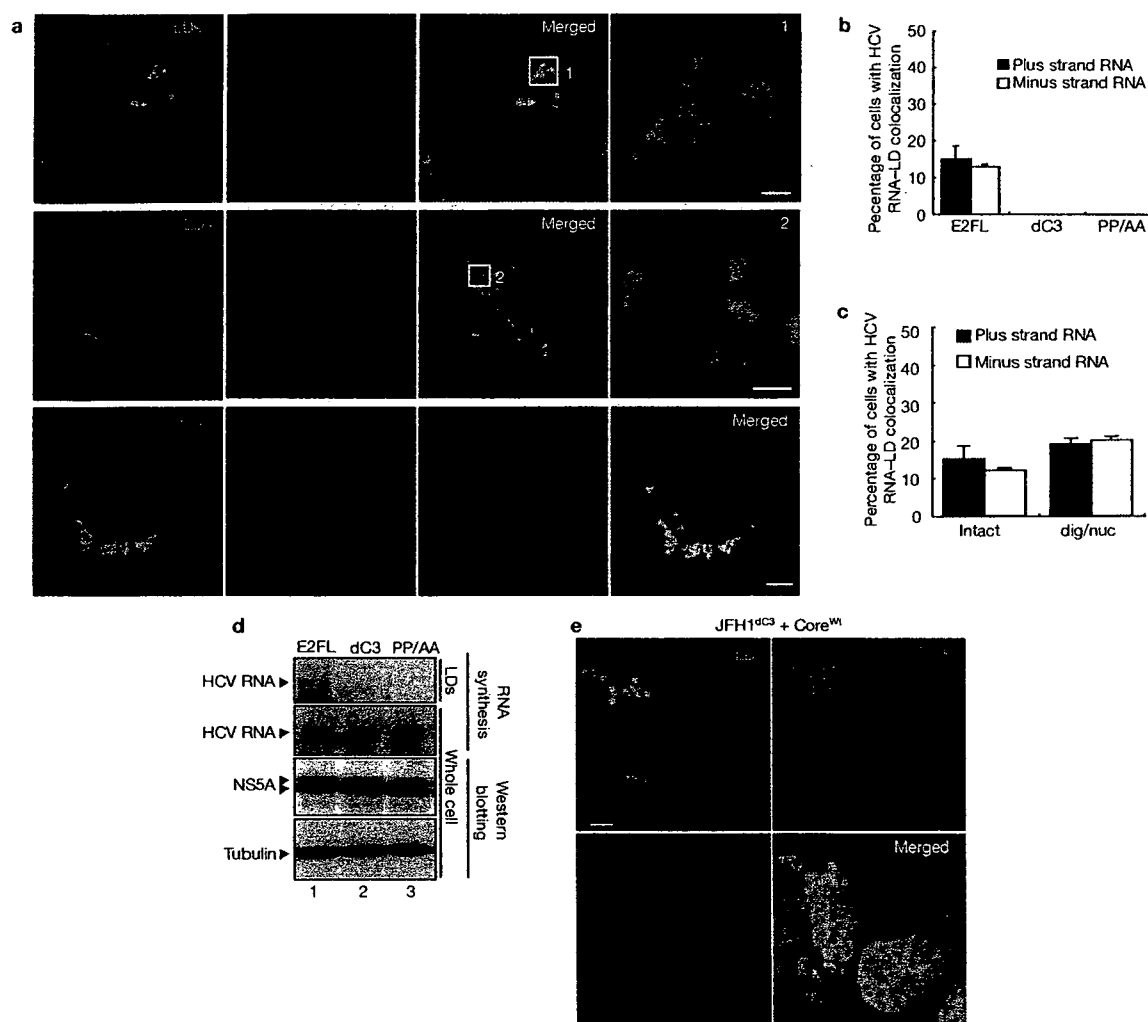


Figure 2 Core-dependent recruitment of active HCV replication complexes to the LD. (a) Huh-7 cells transfected with JFH1^{E2FL} RNA were analysed by *in situ* hybridization with strand-specific probes (plus or minus). The cells were labelled to simultaneously visualize lipid droplets (LDs), NS5A and Core (lower panels). Higher-magnification images of area 1 and area 2 are shown in the upper and middle right panels 1 and 2, respectively. Scale bars: 2 μ m (panels 1, 2); 10 μ m (lower right panel). (b) The percentages of JFH1^{E2FL}-, JFH1^{dC3}- and JFH1^{PP/AA}-expressing cells positive for overlapping signals for LDs and plus- or minus-strand hepatitis C virus (HCV) RNA ($n > 200$). (c) Intact or digitonin and nuclease-treated (dig/nuc) JFH1^{E2FL} replicon-bearing cells were analysed

by *in situ* hybridization. The percentages of cells with overlapping signals for LD and plus- or minus-strand HCV RNA are shown ($n > 200$). (d) RNA-synthesizing activity in the LD fractions purified from cells transfected with JFH1^{E2FL}, JFH1^{dC3} or JFH1^{PP/AA} RNA (top panel). As a control, HCV RNA synthesis activity in digitonin-permeabilized cells was analysed (second panel from the top). HCV protein levels represented by NS5A are shown, together with the level of tubulin (bottom two panels). (e) Localization of plus-strand HCV RNA and Core in JFH1^{dC3} replicon-bearing cells transfected with pcDNA3-Core^{wt} (Scale bar, 10 μ m). Uncropped images of gels are shown in Supplementary Information Fig. S6. All error bars are derived from s.d.

located in the perinuclear region (see Supplementary Information, Fig. S4a). More importantly, in about 20% of these cells, plus- and minus-strand RNAs accumulated around LDs (Fig. 2a, upper and middle panels; 2b) and colocalized with HCV proteins such as Core and NS5A (Fig. 2a, lower panels). No association between HCV RNA and LDs was detected in JFH1^{dC3}- or JFH1^{PP/AA}-replicating cells (Fig. 2b). Northern blot analysis revealed that 4.8% and 5.4% of total plus- and minus-strand HCV RNA, respectively, were detected in purified LD fractions of JFH1^{E2FL}-replicating cells (data not shown). Induction of LD formation with oleic acid did not affect HCV RNA accumulation around LDs (data not shown). These results provide strong evidence that Core recruits HCV RNA as well as NS proteins to LDs.

The HCV replication complex is compartmentalized by lipid bilayer membranes^{16–18}. Therefore, HCV RNA in the complex is resistant to nuclease treatment in digitonin-permeabilized cells¹⁷ (Supplementary Information, Fig. S4b–d). *In situ* hybridization analysis did not reveal a significant difference in the number of cells containing LD-associated HCV RNA before and after nuclease treatment (Fig. 2c), indicating that HCV RNA around LDs is part of the replication complex. An RNA synthesis assay showed that the purified LD fraction from JFH1^{E2FL}-, but not JFH1^{dC3}- or JFH1^{PP/AA}-replicating cells, possessed HCV RNA synthesis activity, even though the expression levels of viral proteins and RNA-synthesizing activities in total cell lysates were similar (Fig. 2d). Moreover, the addition of Core^{wt} rescued the localization of plus- and minus-strand

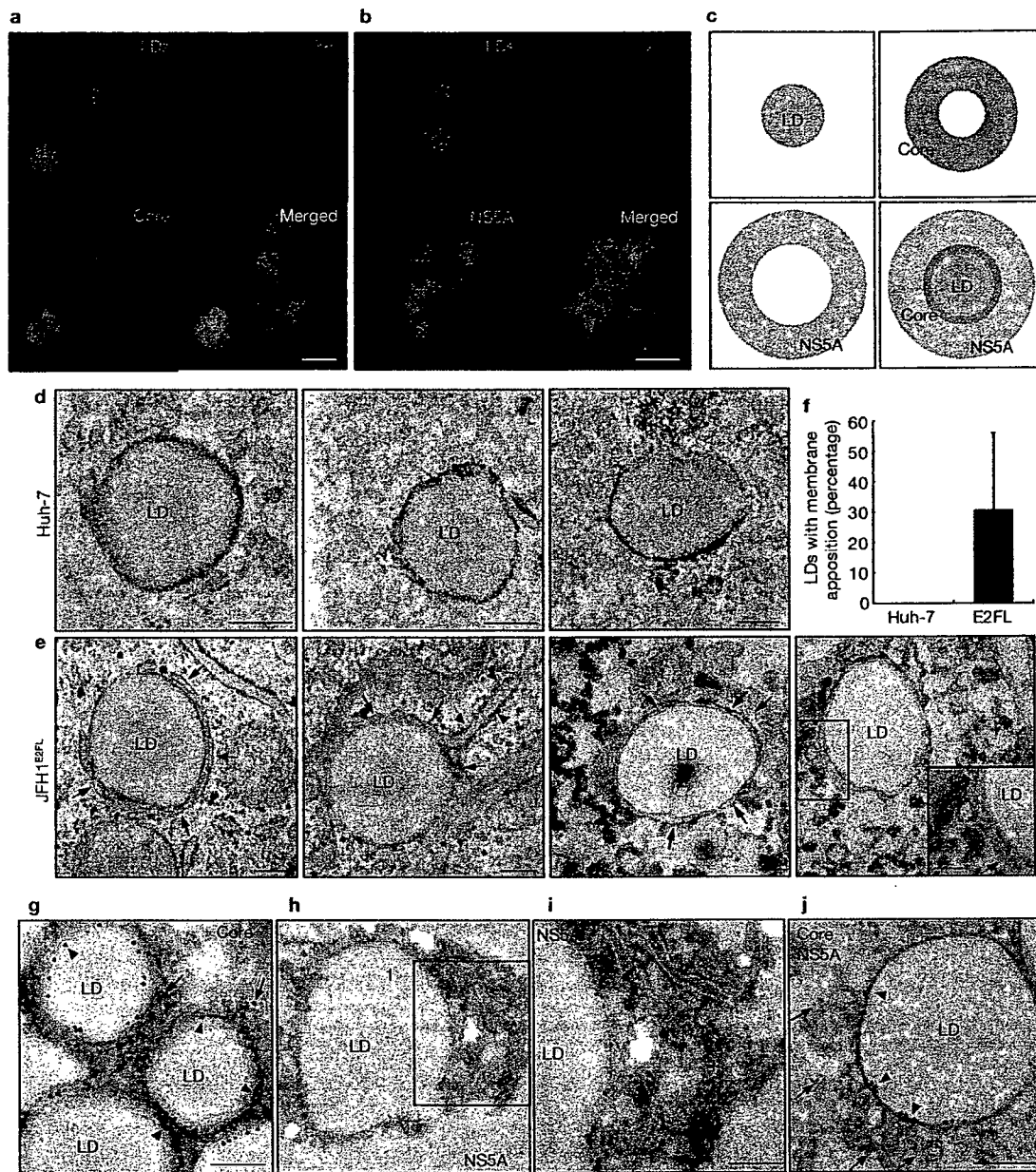


Figure 3 Spatial distribution of Core and NS5A relative to the LD. (a, b) The localizations of Core, NS5A and ADRP around the lipid droplets (LDs) in JFH1^{E2FL} replicon-bearing cells were analysed using immunofluorescence microscopy. Scale bars, 1 μ m. (c) Typical images of the localization of LDs, Core, NS5A and merged images are shown with the relative scale of each image. (d, e) Transmission electron micrographs of LDs in naïve Huh-7 cells and JFH1^{E2FL}-expressing cells. Arrows and arrowheads indicate LD-associated membranes and rough ER membranes, respectively. (f) Frequency of LDs with close appositions

of membrane cisternae. About 100 Huh-7 cells or JFH1^{E2FL}-expressing cells, respectively, were chosen randomly. LDs with apposed membrane cisternae, as exemplified in panel e, were counted as positive. The LDs judged as positive were divided by the total number of LDs.

(g–j) Immunoelectron micrographs of LDs labelled with antibodies against Core (g), NS5A (h, i) or both (j) are shown. Panel i is a higher magnification of area 1 in panel h. In panel j, Core and NS5A are labelled with 15 nm and 10 nm gold particles, respectively. Scale bars, 200 nm. All error bars are derived from s.d.

HCV RNA around LDs in JFH1^{DC3}-replicating cells (Fig. 2e and data not shown). Both plus- and minus-strand RNA associated with LDs were nuclease resistant (data not shown). These results demonstrate that Core recruits biologically active replication complexes to LDs.

The LD is surrounded by a phospholipid monolayer¹⁹, whereas HCV replication complexes are likely to be surrounded by lipid bilayer membranes^{16,17}. Therefore, the replication complexes might not be directly

associated with the membranes of LDs. To characterize the colocalization of LDs, viral proteins and replication complexes more precisely, we analysed the localization of NS5A with high-resolution immunofluorescence microscopy. Core was completely colocalized with ADRP, residing on the surface of LDs²⁰ (Fig. 3a), thus indicating that Core also directly associates with the surface of LDs. More importantly, NS5A mainly localized around the Core-positive area, resulting in a doughnut-shaped signal with a diameter slightly

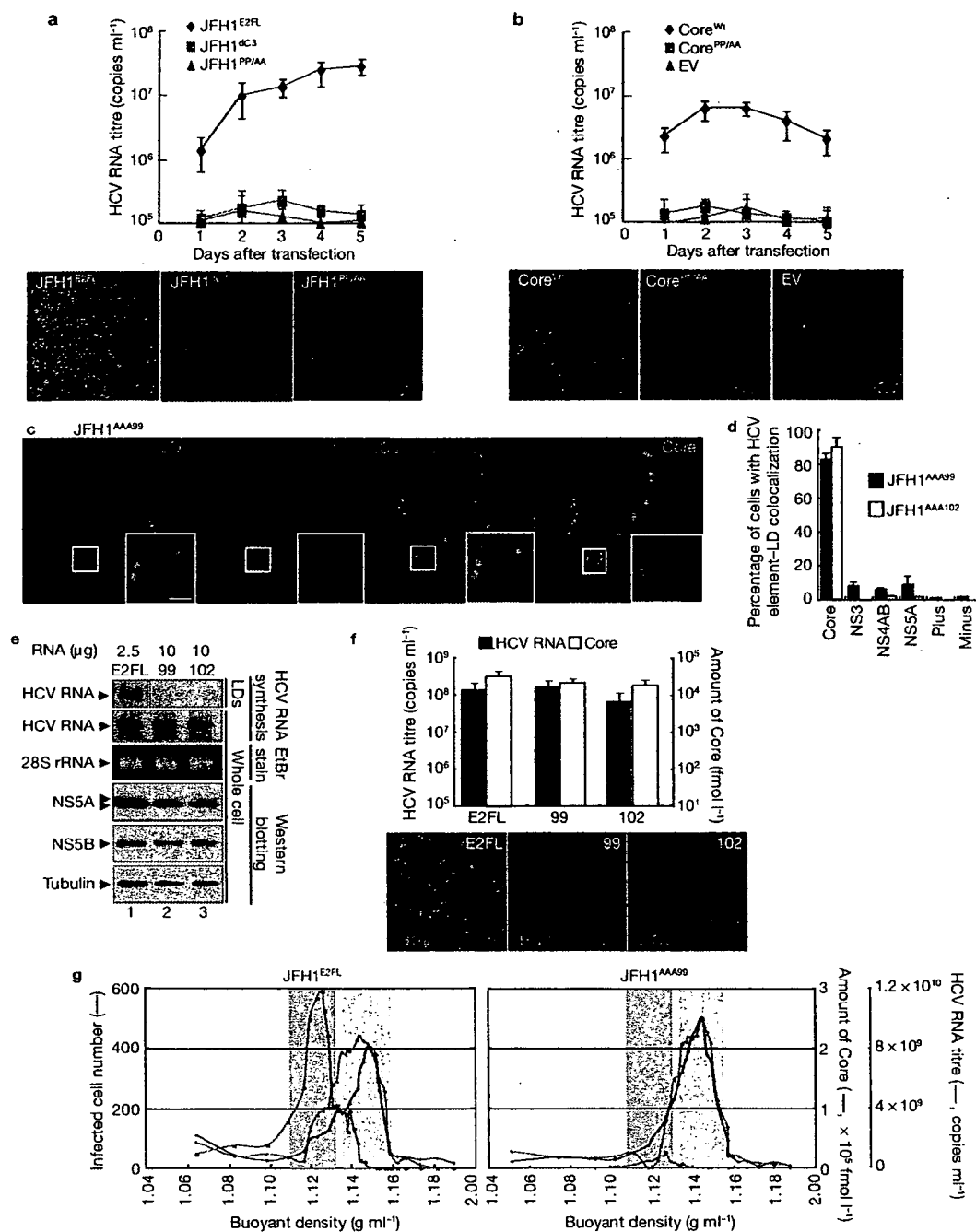


Figure 4 LD associations of Core and NS proteins are necessary for the production of infectious HCV particles. (a) The culture medium from JFH1^{E2FL}, JFH1^{ΔC3}- or JFH1^{PP/AA}-replicating cells was collected at the indicated time points and the titre of hepatitis C virus (HCV) RNA was measured by real-time RT-PCR (upper panel, $n = 3$). The culture medium was added to naïve Huh7.5 cells and, 24 h after inoculation, and cells were labelled with anti-HCV antibodies (lower panels, red). (b) JFH1^{ΔC3} replicon-bearing cells were transfected with pcDNA3 (EV), pcDNA3-Core^{wt} (Core^{wt}) or pcDNA3-Core^{PP/AA} (Core^{PP/AA}). The level of HCV RNA and the infectivity of the culture medium were examined as described above ($n = 3$). (c) Subcellular localization of NS5A and Core in cells expressing JFH1^{AA99}. The insets are high magnifications of the area of the corresponding panel. Scale bar, 2 μm . (d) Percentages of cells in which the signals for given HCV proteins, and plus- and minus-strand HCV RNA, overlapped with those for LDs ($n > 200$). (e) Different amounts of JFH1^{E2FL} (E2FL), JFH1^{AA99} (99) or JFH1^{AA102} (102) RNAs, respectively, were transfected into the same number of

Huh-7 cells. HCV RNA synthesis activity in purified LD fractions (LD) and whole-cell lysates (whole cell) was analysed (HCV RNA synthesis). 28S rRNA was used as a control. Western blot analysis of NS5A, NS5B and tubulin in cells is also shown. All the RNA samples in the top panel were run on the same gel. (f) Analysis of HCV released from cells expressing JFH1^{E2FL}, JFH1^{AA99} or JFH1^{AA102}. HCV RNA titres (black bars) and amounts of Core (white bars) accumulated in the culture medium at 5 d after RNA transfection were measured (upper panel, $n = 3$). Infectivity of the culture medium for naïve Huh-7.5 cells was analysed as described above (lower panels). (g) Concentrated culture medium from JFH1^{E2FL}- and JFH1^{AA99}-replicating cells was fractionated using 20–50% sucrose density-gradient centrifugation at 100,000 g for 16 h. For each fraction, the amounts of Core (black line), HCV RNA (blue line) and infectivity (represented by infected cell numbers in a well; red line) are plotted against the buoyant density (x -axis) ($n = 3$). Uncropped images of gels are shown in Supplementary Information Fig. S6. All error bars are derived from s.d.

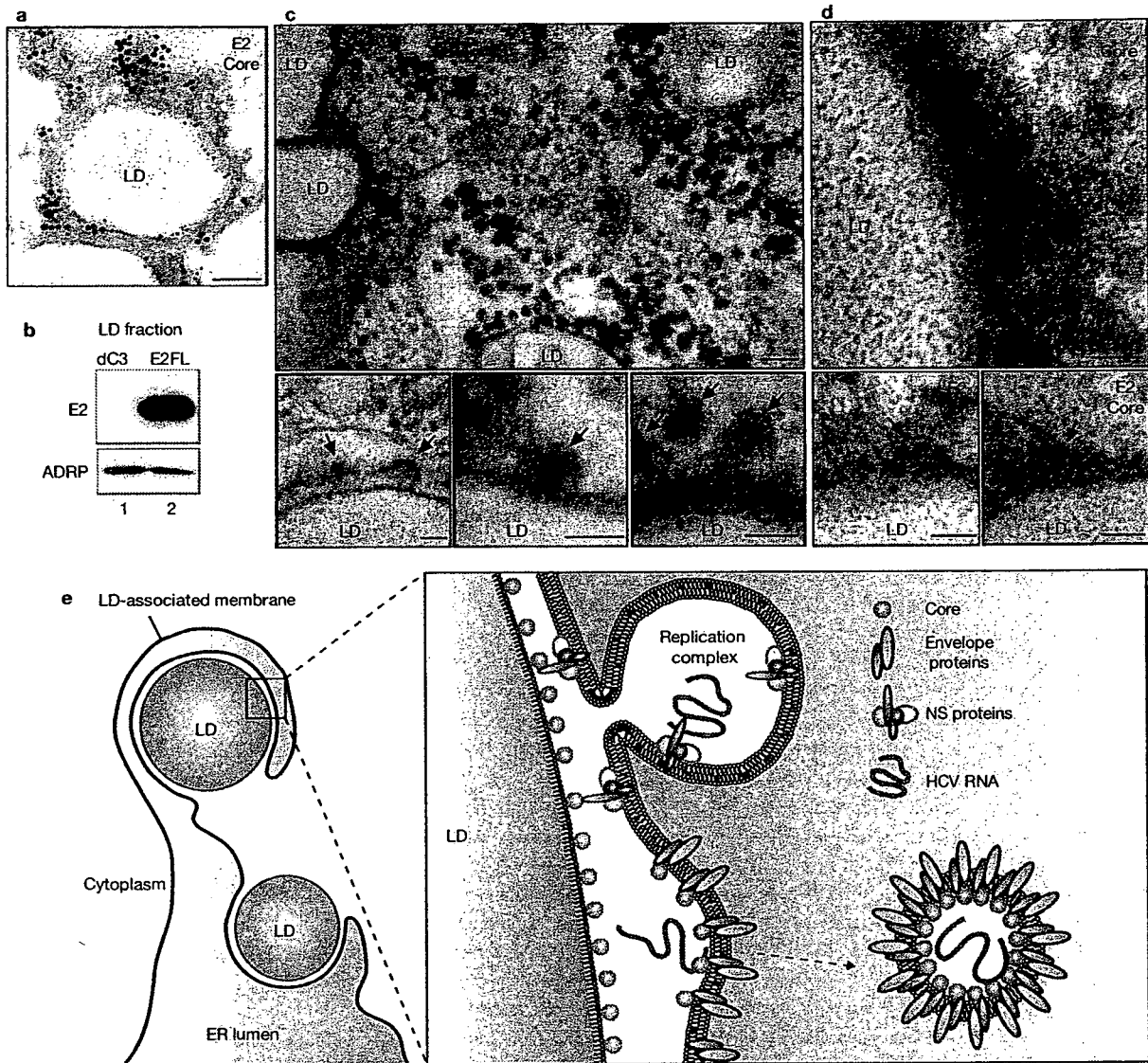


Figure 5 Virus-assembly takes place around the LDs. (a) Immunoelectron microscopic detection of E2 and Core in JFH1^{E2FL}-replicating cells. E2 and Core are labelled with 15 nm and 10 nm gold particles, respectively. (b) Western blot analysis of the lipid droplet (LD) fraction from JFH1^{E2FL} and JFH1^{ΔC3} replicon-bearing cells with anti-E2 and anti-ADRP antibodies. (c) Transmission electron micrographs of JFH1^{E2FL}-replicating cells. Arrows indicate virus-like particles. (d) Immunoelectron micrographs of LDs labelled with antibodies against Core (10 nm) and E2 (15 nm) are shown. Arrows show Core in electron-dense granules. Scale bar: a and upper panel of c: 100 nm;

in d and lower panels of c: 50 nm. (e) A model for the production of infectious hepatitis C virus (HCV). Core mainly localizes on the monolayer membrane that surrounds the LD. HCV induces the apposition of the LD to the endoplasmic reticulum (ER)-derived bilayer membranes (LD-associated membrane). Core recruits NS proteins, as well as replication complexes, to the LD-associated membrane. NS proteins around the LD can then participate in infectious virus production. E2 also localizes around the LD. Through these associations, virion assembly proceeds in this local environment. Uncropped images of gels are shown in Supplementary Information Fig. S6.

larger than that of Core (Fig. 3b). The LD-proximal NS5A signal partially overlapped with the Core signal (Fig. 3b, c, grey). This concentric staining pattern was also observed with the other NS proteins (Supplementary Information, Fig. S5a), indicating that NS proteins associate with Core on the surface of LDs. Electron microscopic analysis only rarely revealed a close association of LDs with other organelles in naïve Huh-7 cells (Fig. 3d, f). However, in the case of JFH1^{E2FL}-replicating cells, about 30% of the LDs were in close proximity to membrane cisternae (Fig. 3e, arrows; 3f), arguing for a HCV-induced membrane rearrangement around LDs. Core was mainly located on the periphery of LDs, and occasionally signals were

observed in more distal areas of the LDs (Fig. 3g, arrowheads and arrows, respectively). Although some NS5A signals were observed on the surface of the LD, the majority of NS5A signals were detected more distal of LDs (Fig. 3h, i). Furthermore, we often observed membrane cisternae as white lines in the same area as NS5A signals (Fig. 3i, arrows). When the same section was labelled with anti-Core and anti-NS5A antibodies, Core was detected on the surface of the LDs, whereas NS5A was mainly observed in the peripheral area of the LDs (Fig. 3j, arrowheads and arrows, respectively). In summary, these results show that Core recruits NS proteins, as well as HCV replication complexes, to the LD-associated membranes.

The above results prompted us to ask whether Core-LD colocalization is important for the production of infectious virus particles. JFH1^{E2FL}-replicating cells released virions into the culture medium and these viruses were highly infectious for naïve Huh-7.5 cells^{11,21}, although culture medium from JFH1^{PP/AA}- or JFH1^{dc3}-replicating cells did not contain significant levels of HCV RNA and infectious virus (Fig. 4a). However, following trans-complementation with Core^{wt}, a high titre of HCV RNA and infectious virus could be rescued from JFH1^{dc3}-replicating cells (Fig. 4b; and see Supplementary Information, Fig. S5b, c). In contrast, the production of infectious viruses was not rescued by trans-complementation with Core^{PP/AA} (Fig. 4b). RNA-binding properties and oligomerization of Core^{wt} and Core^{PP/AA}, which are both necessary for virus assembly, were similar (Supplementary Information, Fig. S5d; ref. 22), arguing that the primary defect of this mutant in preventing infectious virus production is the inability to associate with LDs.

To investigate the contribution of NS proteins around LDs to infectious virus production, we used variants of NS5A, which were not recruited to LDs even in the presence of Core. We assumed that NS5A was crucial for recruiting other NS proteins to LDs, because the level of NS5A recruited to LDs via Core was higher than the levels of the other recruited NS proteins (Fig. 1c, JFH1^{E2FL}). Using alanine-scanning mutagenesis within the NS5A coding region of JFH1^{E2FL}, we generated two mutants, JFH1^{AAA99} and JFH1^{AAA102}, in which the amino-acid sequence APK (aa 99–101 of NS5A) or PPT (aa 102–104 of NS5A) was replaced by AAA (Supplementary Information, Fig. S1). In JFH1^{AAA99}- and JFH1^{AAA102}-replicating cells, NS5A was rarely detected around LDs, whereas Core was still localized to LDs (Fig. 4c, d). Importantly, these mutations impaired not only the NS5A association with LDs, but also the recruitment of other NS proteins and viral RNAs to LDs (Fig. 4d). These results indicate that NS5A is a key protein that recruits replication complexes to LDs. Importantly, HCV RNA synthesis activity in the LD fractions from these mutant JFH1-replicating cells was also severely impaired (Fig. 4e), corroborating the lack of association of HCV replication complexes with LDs.

To investigate the infectious virus production of these NS5A mutants, we prepared cells expressing similar levels of HCV proteins and RNA by adjusting the amount of transfected HCV RNA (Fig. 4e). This was necessary, because replication activities of these mutants were lower compared with JFH1^{E2FL}. Under these conditions, the amounts of Core and HCV RNA that were released into the culture medium from cells transfected with the mutants were comparable to JFH1^{E2FL} (Fig. 4f, upper graph). However, infectivity titres of the mutants were severely reduced (Fig. 4f, lower panels). In sucrose density-gradient centrifugation of culture medium from JFH1^{E2FL}-bearing cells, two types of HCV particles were detected: low-density particles (about 1.12 g ml⁻¹) with high infectivity (Fig. 4g, green area of JFH1^{E2FL}), and high-density particles (about 1.15 g ml⁻¹) without infectivity (yellow area). This result indicates that only a minor portion of released HCV particles is infectious, whereas the majority of released particles lack infectivity. In contrast, cells bearing the JFH1^{AAA99} mutant almost exclusively released non-infectious particles of around 1.15 g ml⁻¹, whereas infectious particles were barely detectable (Fig. 4g, JFH1^{AAA99}). Taken together, these results provide convincing evidence that the association of NS proteins and replication complexes around LDs is critical for producing infectious viruses, whereas production of non-infectious viruses seems to follow a different pathway.

The results described so far imply that some step(s) of HCV assembly take place around LDs. To explore this possibility, we analysed the distribution of the major envelope protein E2 around the LD. Electron microscopic analysis revealed that, in about 90% of JFH1^{E2FL}-replicating cells, E2 was localized in the peripheral area of the LDs (Fig. 5a, large grains). This labelling pattern was similar to the one observed for NS5A (Fig. 3j), indicating that E2 also localizes on the LD-associated membranes. Western blot analysis of the LD fraction supported this conclusion, because the LD fraction that was purified from JFH1^{E2FL}-replicating cells, but not from JFH1^{dc3}-replicating cells, contained E2 (Fig. 5b). Furthermore, spherical virus-like particles with an average diameter of about 50 nm were observed around LDs in JFH1^{E2FL}-replicating cells (Fig. 5c, upper panel). These particles were never observed in naïve Huh-7 cells. A more refined analysis indicates that these particles are closely associated with membranes in close proximity to LDs (Fig. 5c, lower panels, arrows). Finally, these particles around the LDs reacted with Core- and E2-specific antibodies, arguing that the particles represent true HCV virions (Fig. 5d). These results suggest that infectious HCV particles are generated from the LD-associated membranous environment.

In this study, we have demonstrated that Core recruits NS proteins, HCV RNAs and the replication complex to LD-associated membranes. Mutations of Core and NS5A (Fig. 4), which failed to associate with LDs, impaired the production of infectious virus. We note that the mutant Core retains the ability to interact with RNA (Supplementary Information, Fig. S5b) and to assemble into nucleocapsid²². Similarly, the NS5A mutant still supports viral genome replication and the formation of capsids or virus-like particles, arguing that the introduced mutations in Core and NS5A do not affect overall protein folding, stability or function (Fig. 4). Taken together, the data show that the association of HCV proteins with LDs is important for the production of infectious viral particles (Fig. 5e).

Our results also indicate that NS proteins around the LDs participate in the assembly of infectious virus particles. In one scenario, NS proteins may indirectly contribute to the different steps of virus production — for example, by establishing the microenvironment around the LDs that is required for infectious virus production. Alternatively, NS proteins around the LDs may directly participate in virus production — for example, as components of the replication complex that provide the RNA genome to the assembling nucleocapsid.

In support of the role of LDs in virus formation, we observed that colocalization of HCV protein with LDs was low in cases of the chimera Jc1, supporting up to 1,000-fold higher infectivity titres compared with JFH1 (ref. 13). In a Jc1-infected cell, only about 20% of LDs demonstrated detectable colocalization with Core, but this value increased to 80% in the case of a Jc1 mutant lacking most of the envelope glycoprotein genes and thus being unable to produce infectious virus particles (data not shown). This inverse correlation between the efficiency of virus production and Core protein accumulation on LDs indicates that rapid assembly and virus release results in the rapid liberation of HCV proteins from the LDs.

Steatosis and abnormal lipid metabolism caused by chronic HCV infection may be linked to enhanced LD formation¹⁴. In fact, the overproduction of LDs is induced by Core (Supplementary Information, Fig. S3) and HCV also induces membrane rearrangements around LDs (Fig. 3d–f). Our findings suggest that excessive Core-dependent formation of LDs

LETTERS

and membrane rearrangements are required to supply the necessary microenvironment for virus production. NS proteins and HCV RNA seem to be translocated from the ER to the LD-associated membranes. Interestingly, the LD-associated membranes were occasionally found in continuity with ribosome-studded rough ER (Fig. 3e, arrowheads). Thus, at least parts of the LD-associated membranes are likely to be derived from ER membranes. ER marker proteins, however, were not detected in the LD fraction, suggesting that the LD-associated membrane is characteristically distinct from that of ER membranes.

To our knowledge, this is the first report showing that LDs are required for the formation of infectious virus particles. The fact that capsid protein of the hepatitis G virus also localizes to LDs¹⁵ indicates that LDs might be important for the production of other viruses as well. Our findings demonstrate a novel function of LDs, provide an important step towards elucidating the mechanism of HCV virion production and open new avenues for novel antiviral intervention. □

METHODS

Antibodies. The antibodies used for immunoblotting and immunolabelling were specific for Core (#32-1 and RR8); E2 (AP-33 (ref. 23); 3/11, CBH5 and Flag M2 (Sigma-Aldrich, St Louis, MO); NS3 (R212)¹⁷; NS4A and 4B (PR12); NS5A (NSSACL1); NS5B (NS5B-6 and JFH1-1)²⁴; ADRP (Progen Biotechnik, Heidelberg, Germany); tubulin (Oncogene Research Products, MA, USA); Grp78 (StressGen, Victoria, Canada); PDI (StressGen); and Calnexin-NT (StressGen). Antibodies specific for Core (#32-1 and RR8), NS3 (R212) and NS4AB (PR12) were gifts from Dr Kohara (The Tokyo Metropolitan Institute of Medical Science, Japan). Anti-E2 antibody (AP-33) was provided by Dr Patel (MRC Virology Unit, UK). Anti-NS5B (NS5B-6) antibody was kindly provided by Dr Fukuya (Osaka University, Japan). Rabbit polyclonal antibodies specific for NS5A were raised against a bacterially expressed GST-NS5A (1-406 aa) fusion protein. In the case of the HCV chimeras Con1/C3 and H77/C3, immunofluorescence analyses were performed by using the following antibodies: Core (C7/50)⁵, a JFH1 NS3-specific rabbit polyclonal antiserum; NS4B (#86)²⁵; and NS5A (Austral Biologicals, San Ramon, CA).

Indirect immunofluorescence analysis. Indirect immunofluorescence analysis was performed essentially as described previously¹⁷, with slight modifications. Cells transfected with JFH1 RNA were seeded onto a collagen-coated Labtech II 8-well chamber (Nunc, NY, USA). The coating with collagen was performed using rat-tail collagen type I (BD Bioscience, Palo Alto, CA) according to manufacturer's instructions. Three days after seeding, the cells were washed twice with phosphate-buffered saline (PBS; 137 mM NaCl, 2.7 mM KCl, 4.3 mM Na₂HPO₄ and 1.4 mM KH₂PO₄) and fixed with fixation solution (4% paraformaldehyde and 0.15 M sodium cacodylate at pH 7.4) for 15 min at room temperature. After washing with PBS, the cells were permeabilized with 0.05% Triton X-100 in PBS for 15 min at room temperature. For the precise localization of the proteins, the cells were permeabilized with 50 µg ml⁻¹ of digitonin in PBS for 5 min at room temperature²⁶. After incubating the cells with blocking solution (10% fetal bovine serum and 5% bovine serum albumin (BSA) in PBS) for 30 min, the cells were incubated with the primary antibodies. The fluorescent secondary antibodies were Alexa 568- or Alexa 647-conjugated anti-mouse or anti-rabbit IgG antibodies (Invitrogen, Carlsbad, CA). Nuclei were labelled with 4',6-diamidino-2-phenylindole (DAPI). LDs were visualized with BODIPY 493/503 (Invitrogen). Analyses of JFH1 were performed on a Leica SP2 confocal microscope (Leica, Heidelberg, Germany). Analysis of the Con1/C3 and the H77/C3 chimeras was performed in the same way, except that imaging was performed on a Nikon C1 confocal microscope (Nikon, Tokyo, Japan).

Electron microscopy. For conventional electron microscopy, cells cultured in plastic Petri dishes were processed *in situ*. The cells were fixed in 2.5% glutaraldehyde and 0.1 M sodium phosphate (pH 7.4), and then in OsO₄ and 0.1 M sodium phosphate (pH 7.4). The cells were then dehydrated in a graded ethanol series and embedded in an epoxy resin. Ultrathin sections were cut perpendicular to the base of the dish. For immuno-electron microscopy, cells were detached

from the dish with a cell scraper after fixation in 4% paraformaldehyde, 0.1% glutaraldehyde and 0.1 M sodium phosphate (pH 7.4) for 24 h, and washed in 0.1 M lysine, 0.1 M sodium phosphate (pH 7.4) and 0.15 M sodium chloride. After dehydrating the cells in a graded series of cold ethanol, they were embedded in Lowicryl K4M at -20 °C. Ultrathin sections were labelled with primary antibodies and colloidal gold particles (15 nm) conjugated to anti-mouse IgG or anti-rabbit IgG antibodies. For double labelling, colloidal gold particles with different diameters (10 nm and 15 nm) conjugated to anti-mouse IgG or anti-rabbit antibodies were used. Samples were observed after staining with uranyl acetate and lead citrate with a JEM 1010 electron microscope at the accelerating voltage of 80 kV. Anti-Core (#32-1 and RR8), anti-NS5A (NSSACL1) and anti-E2 (Flag M2) antibodies were used.

Preparation of the lipid droplets. Cells at a confluency of ~80% on a dish with a diameter of 14 cm were scraped in PBS. The cells were pelleted by centrifugation at 1,500 rpm. The pellet was resuspended in 500 µl of hypotonic buffer (50 mM HEPES, 1 mM EDTA and 2 mM MgCl₂ at pH 7.4) supplemented with protease inhibitors (Roche Diagnostics, Basel, Switzerland) and was incubated for 10 min at 4 °C. The suspension was homogenized with 30 strokes of a glass Dounce homogenizer using a tight-fitting pestle. Then, 50 µl of 10× sucrose buffer (0.2 M HEPES, 1.2 M KoAc, 40 mM Mg(oAc)₂ and 50 mM DTT at pH 7.4) was added to the homogenate. The nuclei were removed by centrifugation at 2,000 rpm for 10 min at 4 °C. The supernatant was collected and centrifuged at 16,000 g for 10 min at 4 °C. The supernatant (S16) was mixed with an equal volume of 1.04 M sucrose in isotonic buffer (50 mM HEPES, 100 mM KCl, 2 mM MgCl₂ and protease inhibitors). The solution was set at the bottom of 2.2-ml ultracentrifuge tube (Hitachi Koki, Tokyo, Japan). One milliliter of isotonic buffer was loaded onto the sucrose mixture. The tube was centrifuged at 100,000 g in an S55S rotor (Hitachi Koki) for 30 min at 4 °C. After the centrifugation, the LD fraction on the top of the gradient solution was recovered in isotonic buffer. The suspension was mixed with 1.04 M sucrose and centrifuged again at 100,000 g, as described above, to eliminate possible contamination with other organelles. The collected LD fraction was used for western blotting or the HCV RNA synthesis assay.

HCV RNA synthesis assay. An assay of HCV RNA synthesis using digitonin-permeabilized cells was performed as described previously¹⁷. For RNA synthesis assays using the LD fraction, the LD fraction collected by sucrose-gradient sedimentation was suspended in buffer B, which contained 2 mM manganese (II) chloride, 1 mg ml⁻¹ acetylated BSA (Nacalai Tesque, Kyoto, Japan), 5 mM phosphocreatine (Sigma), 20 units/ml creatine phosphokinase (Sigma), 50 µg ml⁻¹ actinomycin D, 500 µM ATP, 500 µM CTP, 500 µM GTP (Roche Diagnostics) and 1.85 MBq of [α-³²P] UTP (GE Healthcare, Little Chalfont, UK), and incubated at 27 °C for 4 h. The reaction products were analysed by gel electrophoresis followed by autoradiography.

Note: Supplementary Information is available on the Nature Cell Biology website.

ACKNOWLEDGEMENTS

We thank T. Fujimoto and Y. Ohsaki at Nagoya University for helpful discussions, and technical assistance. Y.M. is a recipient of a JSPS fellowship. K.S. is supported by Grants-in-Aid for cancer research and for the second-term comprehensive 10-year strategy for cancer control from the Ministry of Health, Labour and Welfare, as well as by a Grant-in-Aid for Scientific Research on Priority Areas "Integrative Research Toward the Conquest of Cancer" from the Ministry of Education, Culture, Sports, Science and Technology of Japan. T.W. is also supported, in part, by a Grant-in-Aid for Scientific Research from the Japan Society for the Promotion of Science; and by the Research on Health Sciences Focusing on Drug Innovation from the Japan Health Sciences Foundation. R.B. is supported by the Sonderforschungsbereich 638 (Teilprojekt A5) and the Deutsche Forschungsgemeinschaft (BA 1505/2-1). M.Z. and R.B. thank the Nikon Imaging Center at the University of Heidelberg for providing access to their confocal fluorescence microscopes and Ulrike Engel for the excellent support.

AUTHOR CONTRIBUTIONS

Y.M. and K.S. planned experiments and analyses. Y.M. was responsible for experiments for Figs 1, 2, 3a-c, 4a-e and 5b. K.A., N.U., electron microscopy; T.H., Fig. 1e; M.Z., R.B., Fig. S2e; and K.S. and K.W., Fig. 4f-g. T.W. provided JFH1 strain. Y.M. and K.S. wrote the manuscript. All authors discussed the results and commented on the manuscript.

COMPETING FINANCIAL INTERESTS

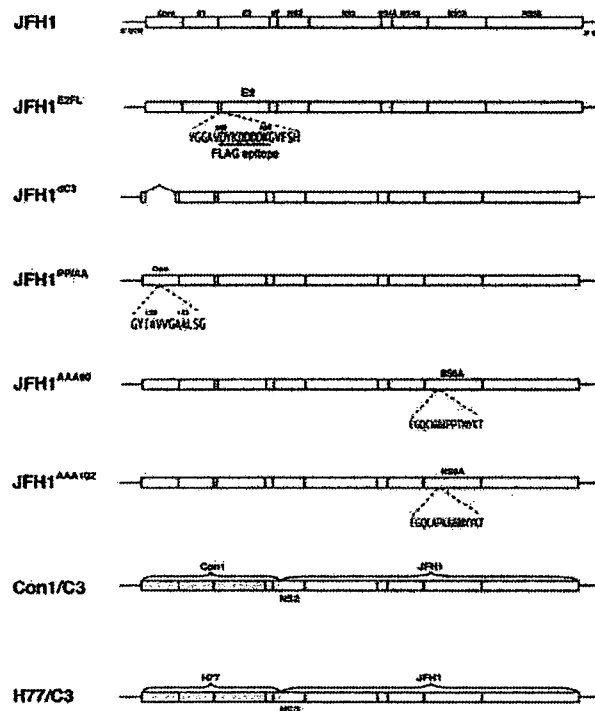
The authors declare no competing financial interests.

Published online at <http://www.nature.com/naturecellbiology/>

Reprints and permissions information is available online at <http://npg.nature.com/reprintsandpermissions/>

1. Martin, S. & Parton, R. G. Lipid droplets: a unified view of a dynamic organelle. *Nature Rev. Mol. Cell Biol.* **7**, 373–378 (2006).
2. Blanchette-Mackie, E. J. *et al.* Perilipin is located on the surface layer of intracellular lipid droplets in adipocytes. *J. Lipid Res.* **36**, 1211–1226 (1995).
3. Vock, R. *et al.* Design of the oxygen and substrate pathways. VI. structural basis of intracellular substrate supply to mitochondria in muscle cells. *J. Exp. Biol.* **199**, 1689–1697 (1996).
4. Liang, T. J. *et al.* Viral pathogenesis of hepatocellular carcinoma in the United States. *Hepatology* **18**, 1326–1333 (1993).
5. Moradpour, D., Englert, C., Wakita, T. & Wands, J. R. Characterization of cell lines allowing tightly regulated expression of hepatitis C virus core protein. *Virology* **222**, 51–63 (1996).
6. Deleersnyder, V. *et al.* Formation of native hepatitis C virus glycoprotein complexes. *J. Virol.* **71**, 697–704 (1997).
7. Kato, N. *et al.* Molecular cloning of the human hepatitis C virus genome from Japanese patients with non-A, non-B hepatitis. *Proc. Natl Acad. Sci. USA* **87**, 9524–9528 (1990).
8. Hijikata, M. & Shimotohno, K. [Mechanisms of hepatitis C viral polyprotein processing]. *Uirusu* **43**, 293–298 (1993).
9. Dubuisson, J., Penin, F. & Moradpour, D. Interaction of hepatitis C virus proteins with host cell membranes and lipids. *Trends Cell Biol.* **12**, 517–523 (2002).
10. Wakita, T. *et al.* Production of infectious hepatitis C virus in tissue culture from a cloned viral genome. *Nature Med.* **11**, 791–796 (2005).
11. Lindenbach, B. D. *et al.* Complete replication of hepatitis C virus in cell culture. *Science* **309**, 623–626 (2005).
12. Zhong, J. *et al.* Robust hepatitis C virus infection in vitro. *Proc. Natl Acad. Sci. USA* **102**, 9294–9299 (2005).
13. Pietschmann, T. *et al.* Construction and characterization of infectious intragenotypic and intergenotypic hepatitis C virus chimeras. *Proc. Natl Acad. Sci. USA* **103**, 7408–7413 (2006).
14. Moriya, K. *et al.* Hepatitis C virus core protein induces hepatic steatosis in transgenic mice. *J. Gen. Virol.* **78**, 1527–1531 (1997).
15. Hope, R. G., Murphy, D. J. & McLauchlan, J. The domains required to direct core proteins of hepatitis C virus and GB virus-B to lipid droplets share common features with plant oleosin proteins. *J. Biol. Chem.* **277**, 4261–4270 (2002).
16. Egger, D. *et al.* Expression of hepatitis C virus proteins induces distinct membrane alterations including a candidate viral replication complex. *J. Virol.* **76**, 5974–5984 (2002).
17. Miyanari, Y. *et al.* Hepatitis C virus non-structural proteins in the probable membranous compartment function in viral genome replication. *J. Biol. Chem.* **278**, 50301–50308 (2003).
18. Quinkert, D., Bartenschlager, R. & Lohmann, V. Quantitative analysis of the hepatitis C virus replication complex. *J. Virol.* **79**, 13594–13605 (2005).
19. Tsuchi-Sato, K., Ozeki, S., Houjou, T., Taguchi, R. & Fujimoto, T. The surface of lipid droplets is a phospholipid monolayer with a unique fatty acid composition. *J. Biol. Chem.* **277**, 44507–44512 (2002).
20. Londos, C., Brasaemle, D. L., Schultz, C. J., Segrest, J. P. & Kimmel, A. R. Perilipins, ADRP, and other proteins that associate with intracellular neutral lipid droplets in animal cells. *Semin. Cell Dev. Biol.* **10**, 51–58 (1999).
21. Blight, K. J., McKeating, J. A. & Rice, C. M. Highly permissive cell lines for subgenomic and genomic hepatitis C virus RNA replication. *J. Virol.* **76**, 13001–13014 (2002).
22. Klein, K. C., Dellos, S. R. & Lingappa, J. R. Identification of residues in the hepatitis C virus core protein that are critical for capsid assembly in a cell-free system. *J. Virol.* **79**, 6814–6826 (2005).
23. Owsianka, A. *et al.* Monoclonal antibody AP33 defines a broadly neutralizing epitope on the hepatitis C virus E2 envelope glycoprotein. *J. Virol.* **79**, 11095–11104 (2005).
24. Ishii, N. *et al.* Diverse effects of cyclosporine on hepatitis C virus strain replication. *J. Virol.* **80**, 4510–4520 (2006).
25. Lohmann, V., Korner, F., Herian, U. & Bartenschlager, R. Biochemical properties of hepatitis C virus NS5B RNA-dependent RNA polymerase and identification of amino acid sequence motifs essential for enzymatic activity. *J. Virol.* **71**, 8416–8428 (1997).
26. Ohsaki, Y., Maeda, T. & Fujimoto, T. Fixation and permeabilization protocol is critical for the immunolabeling of lipid droplet proteins. *Histochem. Cell Biol.* **124**, 445–452 (2005).

Supplementary Figures and legends

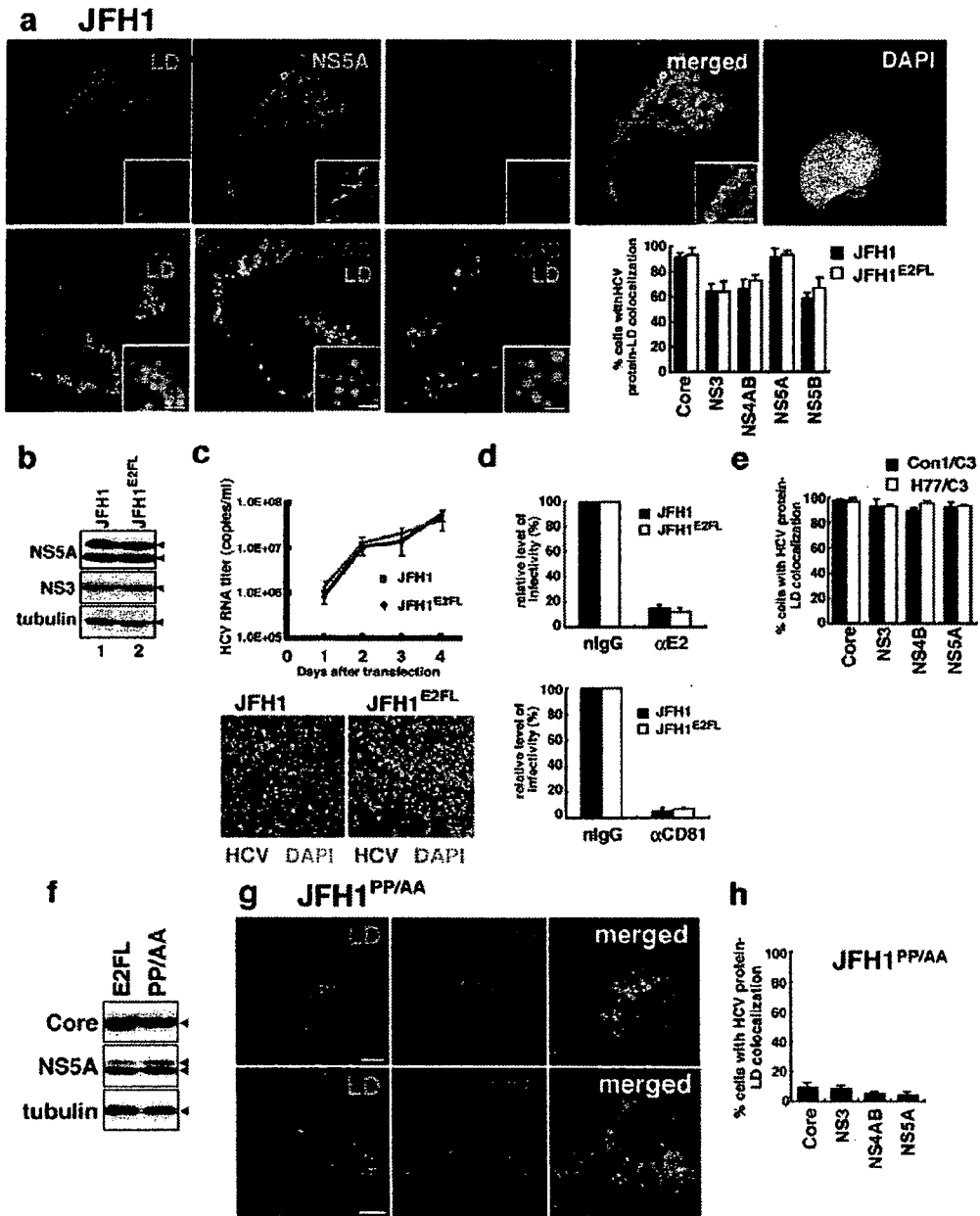


Supplementary Fig. 1

Schematic structures of HCV genomes and mutants used in this study

In JFH1^{E2FL}, the amino acid residues at positions 393 to 400 in the hyper variable region 1 of E2 were converted to a Flag epitope: DYKDDDDK. The JFH1^{E2FL} genome was used to generate other mutant variants of JFH1. In these cases the Flag epitope is marked with a blue vertical line. JFH1^{dC3} carried a deletion in the Core gene that eliminated the 17th to the 163rd amino-acid residue of Core. JFH1^{PP/AA} is a mutant of JFH1^{E2FL} carrying alanine substitutions for proline residues at amino-acid positions 138 and 143 in Core. JFH1^{AAA99} and JFH1^{AAA102} contained mutated NS5A genes carrying triple-alanine substitutions for the APK sequence at amino acid positions 99 to 101 and the PPT sequence at amino acid positions 102 to 104, respectively. Constructs Con1/C3 and H77/C3 are chimeras in which the region from Core to the N-terminal domain of NS2 of JFH1 was replaced by the analogous region of the genotype 1b isolate Con1 or by the genotype 1a isolate H77⁶.

SUPPLEMENTARY INFORMATION



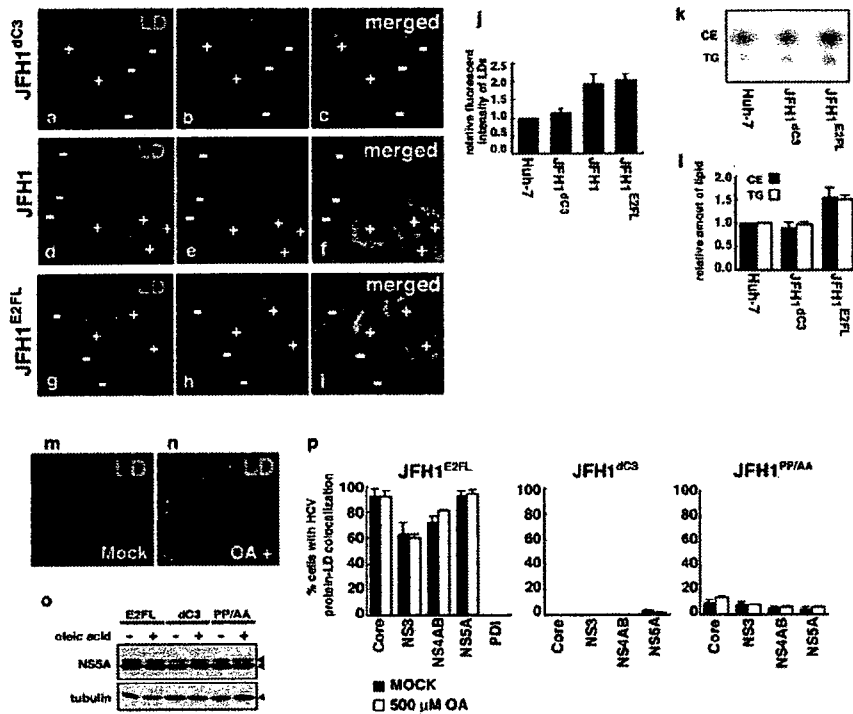
Supplementary Fig. S2 Kunitata Shimotohno
NCB-S11732B

Supplementary Fig. 2 Characterization of mutant JFH1s

(a) JFH1-replicating cells were stained with indicated antibodies, BODYPI 493/503 and

DAPI. Scale bars = 2 μm . Percentages of JFH1- and JFH1^{E2FL}-replicating cells with overlapping signals for LDs and HCV proteins ($n > 200$). (b) HCV proteins in JFH1 and JFH1^{E2FL} replicating cells were analyzed by western blotting with indicated antibodies. (c) Efficiency of virus production and infectivity of JFH1 and JFH1^{E2FL} viruses were analyzed as described in Fig. 4. ($n = 3$) (d) Inhibition of HCV infection by anti-E2 antibody and anti-CD81 antibody. JFH1 and JFH1^{E2FL} virus were pre-incubated with normal IgG (nIgG) or anti-E2 antibody for 1 hr at 4°C and were subsequently used to inoculate Huh-7.5 cells (upper panel). Huh-7.5 cells were pre-incubated with normal IgG (nIgG) or anti-CD81 antibody for 1 hr at 37°C before inoculation with JFH1 or JFH1^{E2FL} viruses (lower panel) ($n = 3$). No obvious difference with respect to the subcellular localization of viral proteins (a), efficiency of viral replication (b), virus production (c), and pathway of virus entry (d) were observed between JFH1^{E2FL} and JFH1 (e) Con1/C3 or H77/C3 replicating cells were stained for HCV antigens (Core or NS3 or NS4B or NS5A) and LDs. The graphs show the percentage of Con1/C3 (black) or H77/C3 (white) positive cells in which HCV protein signals overlapped with LD signals. The overlapping signals were detected by using the ImageJ RG2B software package ($n > 200$). (f) Whole-cell extracts of JFH1^{E2FL} (E2FL) and JFH1^{PP/AA} (PP/AA) replicon-bearing cells were analyzed by Western blot with indicated antibodies. Both Core^{Wt} and Core^{PP/AA} had an apparent molecular weight of about 21 kDa, indicating that Core^{PP/AA} was efficiently processed. The expression level of Core^{PP/AA}, however, was slightly lower than that of Core^{Wt}. (g) Analysis of the subcellular localization of Core and NS5A in cells bearing the JFH1^{PP/AA} mutant. Cells were labeled to detect LDs (green), Core (red), NS5A (red) and nuclei DAPI (blue). Scale bars = 10 μm . (h) The percentages of JFH1^{PP/AA} replicon-bearing cells positive for overlapping signals of LDs and HCV proteins are indicated ($n > 200$).

SUPPLEMENTARY INFORMATION



Supplementary Fig. S3 Kunitata Shimotohno
NCB-S11732B

Supplementary Fig. 3

Enhanced formation of LDs in JFH1- and JFH1^{E2FL}-replicating cells

Cells transfected with JFH1^{dC3} (a-c), JFH1 (d-f), and JFH1^{E2FL} RNA (g-i) were stained with BODIPY493/503 (green), DAPI (blue), and anti-NS5A antibody (red). + and - indicate HCV-positive and HCV-negative cells, respectively. Fluorescence intensities of LDs in Huh-7 cells, JFH1^{dC3}-, JFH1-, and JFH1^{E2FL}-replicating cells were measured by confocal microscopy. The results are represented as relative fluorescence intensity of LDs (j). (k and l) Lipid fraction extracted from Huh-7 cells, JFH1^{dC3}-, and JFH1^{E2FL}-replicating cells was analyzed by thin-layer chromatography. Each lane was loaded with lipid corresponding to an equal amount of protein. Cholesterol ester (CE) and triglyceride (TG) are indicated (k). The relative intensity of CE and TG in panel k is shown in l (n = 3). (m-p) JFH1^{E2FL} replicon-bearing cells were treated with 500 μM oleic acid for 24 hrs and were labeled with BODIPY493/503 (m and n). Cells transfected with JFH1^{E2FL} (E2FL), JFH1^{dC3} (dC3), or JFH1^{PP/AA} (PP/AA) RNA were treated with or without oleic acid. (o) The HCV protein level as represented by the level of NS5A was analyzed by western blot. (p) The percentages of cells positive for overlapping signals for LDs and the HCV proteins or PDI are indicated. The data was obtained in the presence (500 μM) or absence (MOCK) of oleic acid in the culture medium (n > 200).